Ecological network structure in response to community assembly processes over evolutionary time

Ecological networks and community assembly

Natalie R. Graham[1*], Henrik Krehenwinkel[2], Jun Ying Lim[3], Phillip Staniczenko[4], Jackson Callaghan[5], Jeremy C. Andersen[6], Daniel S. Gruner[7], Rosemary G. Gillespie[1]

[1] Department of Environmental Sciences Policy and Management, University of California Berkeley, Mulford Hall, Berkeley, California, USA

[2] Department of Biogeography, Trier University, Faculty of Regional and Environmental Sciences, Trier 54286, Germany

[3] Department of Biological Sciences, National University of Singapore, Singapore

[4] Department of Biology, Brooklyn College, City University of New York, USA

[5] Department of Integrative, Structural and Computational Biology, The Scripps Research Institute, San Diego, California, USA

[6] Department of Environmental Conservation, University of Massachusetts Amherst, Amherst, Massachusetts, USA

[7] Department of Entomology, University of Maryland, College Park, Maryland, USA

*Corresponding author

Email: n.graham@berkeley.edu

Abstract

The dynamical structure of ecological communities results from interactions among taxa that change with shifts in species composition in space and time. However, our ability to study the interplay of ecological and evolutionary processes on community assembly remains relatively unexplored due to the difficulty of measuring community structure over long temporal scales. Here, we made use of a geological chronosequence across the Hawaiian Islands, representing 50 years to 4.15 million years of ecosystem

development, to sample 11 communities of arthropods and their associated plant taxa using semi-quantitative DNA metabarcoding. We then examined how ecological communities changed with community age by calculating quantitative network statistics for bipartite networks of arthropod-plant associations. The average number of interactions per species (linkage density), ratio of plant to arthropod species (vulnerability), and uniformity of energy flow (interaction evenness) increased significantly in concert with community age. The index of specialization H_2' has a curvilinear relationship with community age. Our analyses suggest that younger communities are characterized by fewer but stronger interactions, while biotic associations become more even and diverse as communities mature. These shifts in structure became especially prominent on East Maui (~0.5 my) and older volcanos, after enough time had elapsed for adaptation and specialization to act on populations *in situ*. Such natural progression of specialization during community assembly is likely impeded by the rapid infiltration of non-native species, with special risk to younger or more recently disturbed communities that are composed of fewer specialized relationships.

Keywords community assembly, ecological networks, DNA metabarcoding, oceanic islands

Introduction

Biodiversity is organized into complex ecological networks of interacting species that change through time in response to ecological and evolutionary processes. Understanding these changes is important for predicting the impacts of global change on higher multispecies organization (Dell et al., 2019; Smith-Ramesh et al., 2017; Staniczenko et al., 2017). A suite of analytical tools (Delmas et al., 2019) exist to quantify changing community structure in response to a variety of perturbations (Aizen et al., 2008; Fricke et al., 2017; Vacher et al., 2010). A major challenge remaining is to understand the configuration of ecological networks in a predictive context over long spatiotemporal scales (Poisot et al., 2015; Trøjelsgaard & Olesen, 2016; Yeakel et al., 2014). Consequently the effect of community assembly processes on the structure of interaction networks describing ecological communities remains poorly understood (Ponisio et al., 2019; Rominger et al., 2016).

Early research on community assembly often ignored ecological interactions due to their complexity. Notably, neutral models for community assembly are even agnostic to organismal identity (Hubbell, 2001; Rosindell et al., 2011). As species identity and interactions began to be incorporated into models, the initial ‘assembly rules’ of Diamond (1975) highlighted 'forbidden species combinations' and nonrandom patterns of co-occurrence. A growing recent theme focuses on the effect of abiotic and biotic filters on a regional species pool (Münkemüller et al., 2020) with varying temporal and spatial filters dictating network structure (Peralta et al., 2019). However, much of this work ignores the role of evolution in shaping interactions through time. The extent of adaptation, and possible speciation, in shaping interactions as communities assemble, depends on the isolation of the community from the source pool (Gillespie et al., 2020; Rosindell & Phillimore, 2011). At the extreme, evolution will have shaped interactions among every member of a community and the effects of filtering from a regional species pool might thus appear relatively weak (Ponisio et al., 2019). While most communities will include the role of both ecological filtering and evolutionary adaptation, our ability to thread complex ecological questions of network structure into an evolutionary framework has presented a major obstacle.

Recognizing this impediment, recent work has examined avenues to approach the problem. In particular, models of trait evolution on phylogenies provide a means to understand how eco-evolutionary feedbacks shape interactions as communities assemble (Segar et al., 2020). Likewise, based on theory showing how change across short time scales affects longer-term evolutionary dynamics, clade-level phylogenetic comparative approaches can be applied to community data to understand the dynamics of network structure (Weber et al., 2017). Both these approaches focus on the lineages that make up communities, asking how interacting sets of lineages affect each other. However, another approach is to focus explicitly on the community rather than individual lineages, connecting large-scale understanding of community interactions at a given time period in a spatially variable environment with the understanding of how the integrated structure of biodiversity changes through time. Such an approach attempts to address a major gap in the field by bridging macroecology and macroevolution (McGill et al., 2019) and hence showing how network structure changes across scales of space and time within a whole-community context (Weber et al., 2017).

While theory indicates a clear role for biotic interactions leading to individual and community specialization over long-term community development, empirical evaluation has been challenging. One difficulty is in obtaining measures of community composition and interactions at relevant spatial scales, and another obstacle is the vast timeframe over which evolutionary phenomena occur. With their short generation times that are amenable to laboratory studies, microbial systems provide exceptional cases that document community assembly over evolutionary time scales (Boon et al., 2014; Koskella et al., 2017; Koskella & Brockhurst, 2014; Venturelli et al., 2018). In particular, studies of the plant phyllosphere showed a more prominent role of nonneutral selection over time and an increase in the strength of biotic interactions and community cohesion (Morella et al., 2020). However, to infer the role of interactions in community assembly of longer-lived macroorganisms requires very particular systems. Here, we make use of two sets of circumstances that, together, provide an extraordinary opportunity to assess the nexus of ecological and evolutionary community assembly in the context of interaction networks.

First, we use the system provided by the Hawaiian Islands. Islands in general provide discrete communities that can be used for natural experiments in interaction dynamics (Brodie, 2017; Castro-Urgal & Traveset, 2014; Olesen et al., 2002). In particular, oceanic archipelagos formed *in situ* over millions of years offer the opportunity to study species interactions over evolutionary timescales (Hembry et al., 2018; Ponisio et al., 2019; Rominger et al., 2016; Trøjelsgaard et al., 2013). Moreover, the geological series of islands in the Hawaiian archipelago represents a chronosequence (Vitousek, 2002; Walker et al., 2010); each substrate age represents communities of different ages, ranging from ~ 50 years to ~ 5 Myr (Shaw & Gillespie, 2016). Notably, the native montane forest of Hawaii is dominated by just two canopy tree species (*Metrosideros polymorpha* and *Acacia koa)*, making it relatively simple ecologically and hence more amenable to capturing and characterizing whole communities.

Second, we make use of the emerging field of DNA metabarcoding (Krehenwinkel, Wolf, et al., 2017; Yu et al., 2012), which makes a comprehensive analysis of taxonomic composition possible, offering the opportunity to simultaneously assess thousands of species rapidly, offering enormous potential for reconstructing complex ecological networks (Clare, 2014; Hrček & Godfray, 2015; Vacher et al., 2016). Relative sequence abundances offer a proxy for interaction strength (Lim et al., 2021), providing greater reliability for co-occurrence studies to measure biotic associations (Bálint et al., 2018; Mata et al., 2021). Combining high-throughput sequencing with theoretical approaches, such as statistical modeling (Faust & Raes, 2012; Newman & Girvan, 2004) and machine learning (Bohan et al., 2011), shows considerable promise in helping to close the gap on the historical impediments for comprehensive quantification of interactions in ecological communities.

Here we use semi-quantitative DNA metabarcoding to build networks of arthropod-plant associations at 11 sites across the Hawaiian chronosequence, using the substrate age at a site as measure of community age, and then use those networks to test a range of expectations on how ecological and evolutionary processes shape community structure over long timescales (e.g., Table 1). We expect network size - both the number of nodes and number of links - will increase with community age, but disproportionately, as younger communities gain taxa through colonization only and older communities

assemble through colonization and evolutionary processes. This allows tests of the following hypotheses for evolutionary assembly of networks (Figure 1): (H1) Starting from bare lava, early successional communities offer low resource diversity yet are necessarily composed of assemblages from nearby species pools. Therefore, younger communities will have a high proportion of generalists – a subset of the nearby species pool most likely to persist without particular interaction partners – but greater interaction frequency on fewer interaction pathways because of resource heterogeneity. (H2) The set of biotic interactions that a given taxon will experience will decrease with community age, and the evenness of the interactions among resources will increase, resulting in greater network specialization (Ponisio et al., 2019; Rominger et al., 2016). One ideal component of this study is the large temporal span of time for community assembly. We can assume that younger communities will gain taxa only through colonization given that they are not established long enough for *in situ* speciation to take place. Of course, older communities will assemble through colonization and evolutionary processes. We cannot tease apart the effects of both processes at the oldest sites, but we can compare the youngest to oldest sites and their related ecological networks for signatures of assembly after evolutionary processes have taken effect. With an increasing number of taxa that have evolved together in a community it follows there will also be an increase in the specialization of the interactions among these species that may be detectible at the network architecture level.

Materials and Methods

Site selection methods

The Hawaiian Islands are formed as the Pacific plate moves northwestward across a stationary volcanic hotspot, therefore the archipelago represents a chronosequence of geological age from the youngest island (Hawaii, ~0–0.5 Myr), to the oldest high island of Kauai (~5 Myr), (Clague, 1996). Discrete volcanoes within islands present additional contrasts in geological age, and the underlying substrate age has been mapped in fine detail (Wolfe & Morris, 1996). *Metrosideros polymorpha* (Myrtaceae) is the dominant canopy tree in these forests across islands, with patches of sub-dominant *Acacia koa* (Fabaceae) and numerous associated understory trees, shrubs, herbs, and ferns (Gagne & Cuddihy, 1990).

153

154 We selected 14 sites of varying geologic age, ranging from 50 to 4.15 x 10^6 years old, across four islands
155 of the archipelago: Hawaii, Maui, Molokai, Kauai (SI Figure 1, SI Table 1). To control for climatic
156 differences and disturbance across sites, sites were constrained to ranges of elevation (1000-1300 m)
157 and precipitation (average annual precipitation 2500-3000 mm) and within accessible protected forest
158 lands (*Gap Analysis Project | U.S. Geological Survey*, 2019; Giambelluca et al., 2013).

159

160 For each potential site, spatial polygons were created based on the intersections of these layers and
161 initial field reconnaissance to confirm remotely sensed data and feasibility of access. Within these
162 potential site polygons, airborne high-resolution laser scanning from the Global Airborne Observatory
163 (GAO; formerly named Carnegie Airborne Observatory; Asner et al. (2012)) was used to generate forest
164 canopy height profiles using a physical model described in Asner et al. (2008). The ground digital
165 elevation model was also generated using the method of Asner et al. (2007). The data were collected at
166 4 laser shots per square meter, processed to height profiles at 5 m resolution and then averaged at a grid
167 cell spacing of 30 m (SI Figure 2 and SI Table 2).

168

169 20 randomized candidate plots were generated for each site, with the intention of ultimately selecting six,
170 15 m-radius plots. These 20 randomized candidate plots were constrained to be a minimum distance of
171 200 m from all other plots and to be within the top 40% quantile of LiDAR-estimated canopy heights.
172 Candidate plot generation was achieved with custom scripts in the R programming language (R Core
173 Development Team, 2019) using a simple rejection sampling algorithm: random sets of spatial locations
174 are generated within pixels of sufficient canopy height until a set of locations is found which meet the
175 requirement of being 200 m distant. The minimum distance of 200 m was a constraint to maximize
176 independence among sampling areas while capturing more spatial heterogeneity within sites.

177

178 At each site, each of the 20 candidate plots were ground-truthed to confirm the plot was dominated by
179 native vegetation and minimally impacted by human use and/or invasive vertebrates. This ground-truthing
180 process eliminated a variable number of the initial 20 candidate plots. If fewer than six final plots

remained after ground-truthing, another set of candidate plots were generated and ground-truthed to find a final set of six plots. If more than six plots remained after ground-truthing, the final six plots were selected by randomly selecting from the ground-truthed plots.

Collection protocol

We collected arthropods using vegetation beating at six 15 m radius plots per site during May 2015 through January 2016, with plots sampled randomly to avoid seasonality effects on arthropod composition. To ensure equal sampling effort across sites, sampling was limited to a total of 420 seconds in each plot. If after all arthropod collection processing steps (described below) the total vegetation beating time for a plot was not within one standard deviation of 420 seconds sampling effort then that plot was dropped from further analyses, resulting in a total of 50 plots from 11 sites (SI Table 1). As we were interested in characterizing plant-arthropod associations, we sampled plant genera in each plot proportional to their relative abundance. Percentage cover of each understory plant genus was estimated visually. Where plants could not be identified to the genus-level, we grouped them into morphotaxa and sampled them accordingly. Vegetation beating was performed by placing 1 m x 1 m white beating sheets under individual plants and gently agitating the foliage using a one meter length pvc pole for timed second intervals. Arthropods dislodged by the agitation which drop onto the beating sheet are aspirated into a vial containing 95% ethanol. Each plant associated arthropod community sample was transferred to one or more 2 ml vials containing fresh 95% ethanol, labeled, and transported to the lab where it was stored at -20 °C.

Specimen sorting and DNA extraction

To reduce bias due to differently sized individuals contributing disproportionate amounts of DNA (Elbrecht & Leese, 2015) specimens were sorted following procedures described in Lim et al. (2021). Each plant beating sample was sorted in petri dishes on 1 mm graph paper under a stereoscope into four size categories (0-2 mm, 2-4 mm, 4-7 mm, 7 mm and up) based on the body size distribution found in a common Hawaiian ecosystem. Individuals in each size category were counted and placed with fresh

ethanol into a single well in a 96-well plate. Thus, all individuals from a particular plant genus at a particular plot have their DNA extracted together and are prepared together using a dual-indexing strategy described below into NGS amplicon libraries for sequencing. The Collembola had considerably higher abundance than the remaining arthropods in the small size categories, therefore Collembola were separated into 1.5 ml Eppendorf tubes and processed for DNA extraction and sequencing parallel to the remaining arthropod community samples.

Specimens from public and private collections were also used to generate a DNA barcode reference library for 57 species. We used whole bodies of species from private collections where available because these were easiest to generate sequences from preserved material (86% barcode generation success). Genomic DNA extraction of size sorted arthropod-plant community samples was performed in 600 µl volumes using the Tissue protocol described in the Qiagen Puregene kit modified for automation (Lim et al., 2021). DNA was eluted in 50 ul DNA Hydration Solution.

Sequence analysis

Each size sorted sample and a PCR negative for each 96 well plate (containing no template DNA) was amplified with a primer combination (ArF1/ Fol-degen-rev) (Gibson et al., 2014; Yu et al., 2012) that targets a 418 bp fragment in the barcode region of the Cytochrome Oxidase I (COI) gene. This primer pair has been suggested as the most appropriate for capturing arthropod diversity in DNA metabarcoding studies (Elbrecht & Leese, 2015) and has been shown to reliably amplify the Hawaiian arthropod community (de Kerdrel et al., 2020). PCRs were run in 10 µl volumes using the Qiagen Multiplex PCR kit at an annealing temperature of 46 °C, with 1 µl of DNA and 0.5 µl of each 10 µM primer. A first round of PCR consisted of 32 cycles using tailed primers; each primer additionally had a unique 6 bp inline barcode so that multiple plates of the same primer can be pooled together. PCR products were cleaned of residual primer using a 1x ratio of SPRI beads (Sera-Mag™) and pooled together based on band intensity (i.e., DNA concentration) on an agarose gel relative to a DNA ladder (NEB) and using the Gel Doc XR System with the Quantity One software (Bio-Rad). A second indexing PCR of 6 cycles was performed with the pooled amplicons to introduce dual indexes and Illumina® TruSeq sequencing

adapters to 5′-tails of the locus-specific PCR primers (Lange et al., 2014), with a final 5'-3' layout as Illumina adapter, 6 bp inline barcode, PCR primer as described in de Kerdrel et al. (2020). The indexed products were cleaned again with SPRI beads, quantified by electrophoresis, and then pooled in equal amounts into a single tube. The samples were then sequenced on an Illumina® MiSeq using V3 (600 cycles) chemistry according to the manufacturer's protocol (Illumina, San Diego, USA). We aimed for a total of 30,000 reads per sample. Each PCR negative was sequenced with each plate of specimen libraries regardless of the absence of detectable PCR product on a gel.

We generated 2276 metabarcode libraries with each library representing the total arthropods collected for each plant genus for each plot (a sampling event), sorted into one of four size categories (a sequencing pool). Sequences were demultiplexed on Illumina® BaseSpace by sample well based on the two 8-bp indexes with no mismatches allowed. We merged paired reads using PEAR (Zhang et al., 2014) with a minimum overlap of 50 bp and a minimum quality of Q20. Merged reads were quality filtered (≥90% of bases ≥Q30) and transformed into fasta files using the FastX Toolkit (Gordon & Hannon, 2010). The resulting fasta files were demultiplexed by PCR primer and 6 bp inline barcode combination, using the forward and reverse primer sequences as indices with the grep command in UNIX, and the primer sequences were then trimmed using the UNIX stream editor.

Rarefaction and pseudogene removal

We rarefied each sample using a custom unix command that drew from the total reads of the metabarcoding analysis a number of reads that was equivalent to the numerical abundance of individual arthropods counted into each well of the 96-well plate, repeating the draw of sequences 100 X with replacement. The process of rarifying by repeated random draw based on the expected individual specimen abundance should correct the disproportionate abundance of sequences that accumulate for larger specimens compared to smaller specimens, due to the amplification bias that is inherently caused by differential starting tissue amounts (Lim et al., 2021).

We generated zero-radius OTUs (zOTUs), from the rarefied raw reads with the unoise3 command (Edgar, 2016) following the recommended protocols in the USEARCH v11 pipeline (Edgar, 2010). Specifically, the quality trimmed reads were dereplicated and clustered into zOTUs using the unoise3 command in USEARCH. Chimera were removed *de novo* in USEARCH. The resulting zOTUs were compared against the NCBI Genbank database and our custom-made DNA reference library for Hawaiian taxa using BLASTn with a maximum of 10 target sequences. All non-arthropod zOTUs were removed after which 5,046 zOTUs remained. We aligned these 5046 zOTUs using default settings in Clustal Omega (Sievers et al., 2011). To remove putative pseudogenes from the zOTU dataset we ran metaMATE with default specifications and the example specifications file to detail how per-zOTU read frequencies should be assessed (Andujar et al., 2021). Using the output of metaMATE we applied the least stringent Numt removal strategy so that we could retain as many putatively true zOTUs as possible (Graham et al., 2021), this reduced the number of zOTUs from 5046 to 4330.

Taxonomic matching and abundance estimates

About a quarter of the zOTUs (*n* = 901) were matched to the Blast or voucher DNA reference library with less than 85 percent similarity. To validate the taxonomic identification for each zOTU at higher taxonomic levels (e.g. order, family) we compared the top 10 blast and reference library hits with phylogenetic clustering from a ML tree. A ML tree with bootstop autoMRE bootstrap support was generated by running RAxML-HPC v.8 on XSEDE on the Cipres science gateway (Miller et al., 2010) under the GTR model with a gamma distribution plus invariant sites. For 28 zOTUs taxonomic order could not be determined via sequence similarity to databases or phylogenetic clustering and were thus removed from downstream analysis. Taxonomic assignment was considered trustworthy if the percent similarity of the metabarcoding sequence to the NCBI GenBank or DNA reference voucher was: between 88-94% for family, between 94%-98% for genus and greater than 98% percent similarity for species, while matches below 88% similarity were made only to order. These threshold values were arbitrarily chosen based on previous investigations using mock communities or photo voucher integrative taxonomy of select taxa from the same high-elevation wet forest communities of Hawaiian arthropods and amplified using the same COI marker (Krehenwinkel et al. 2017, de Kerdrel et al. 2020).

To create a table with OTU abundances for community analyses we mapped a query set of raw reads to the filtered and taxonomically identified search database of zOTUs in USEARCH v11 (Edgar, 2010) using the otutab command with the default 97% percent similarity mapping threshold. After OTU mapping and read removal based on the PCR negative control sequencing pool the number of unique sequences was reduced by 133 zOTUs to 4197 OTUs.

In order to use relative sequence abundance of arthropod OTUs as an approximation of arthropod-plant associations, we adopted a semi-quantitative processing pipeline (Lim et al., 2021) to ameliorate differences in sampling effort, body size of specimens, and genomic procedures. To review, (1) for each site (community) there was six plots, (2) within each plot each plant taxon was sampled by seconds of time corresponding to its relative abundance in the plot, (3) we sorted bulk arthropod samples by size and counted the individuals, (4) sequences were generated using a DNA region with demonstrated success for Hawaiian arthropod taxa (de Kerdrel et al., 2020) and false reads (pseudogenes) were removed (Graham et al., 2021), (5) we randomly sampled the sequencing reads based on the count of individuals in each size class, and finally, (6) sequence reads were summed across size classes and plots (Figure 1b).

Calculation of quantitative ecological network metrics

Using bipartite networks of arthropod-plant associations at each community age, we tested our hypotheses by calculating quantitative (weighted) and qualitative (binary) network metrics (Table 2) expected to occur in the transition from younger communities to older communities (Table 1). Data processing and statistical analyses were performed in R version 4.0.2. To distinguish between taxa that have colonized the archipelago historically or more recently, we characterized the probable native and non-native composition for each aged community based solely on sequence characteristics as outlined in Andersen et al. (2019). The approach considers both the evolutionary distances between species and the genetic diversity within species. Sequence characteristics of OTUs show a higher amount of neutral (or

otherwise) sequence variation among endemic taxa, as they have evolved from a common ancestor on the islands, when compared to non-native taxa that evolved elsewhere and have no close relatives. The approach was implemented into a machine learning strategy using random forests in sklearn and packaged with multiple utilities and a graphical user interface in NIClassify (https://github.com/tokebe/niclassify). By annotating the nativeness status for sequences which are identifiable to species level (98% or above match to databases), NIClassify can accurately assign status for the remaining sequences. As part of the NIClassify classifications an output of accuracy is obtained by withholding species with known statuses during the training, and then comparing the results for those samples based on the classifications. These samples are randomly selected by the program, so biases in regards to well- versus under-sampled taxa are not expected to influence the training.

We aggregated the sequence abundance for each arthropod OTU according to its association with a particular plant genus within a site. For example, we found the sum of the sequence abundances for OTU 'X', a Hemiptera from genus *Nesodyne*, that was associated with (i.e., collected on) plants in the genus *Coprosma*. We configured the arthropod-plant abundance data as a matrix with arthropods as columns and plants as rows; there were 11 matrices, one for each site of different substrate age. As such, we measure the strength of an interaction as the sequence abundance of the arthropod that was collected on a particular plant species, as it is an aggregated assessment of the arthropod-plant association across multiple plants and multiple plots within a site. We also graphed quantitative and qualitative metrics for matrices of arthropod-plant interactions at each plot within a site. However, we constrain our discussion to the aggregated network data because our confidence in the network statistics increases with the size of the networks. This was a particular issue for some plots at the youngest and most depauperate sites, where < 4 plant species were sampled within the plot radius and networks would be small.

We plotted the ecological network matrix for each community age using the 'plotweb' command in the R package bipartite. For each network, lower bars represent plant abundance based on sampling time and upper bars represent arthropod abundance based on OTU frequency. For visual simplicity, we grouped upper bars by arthropod order. As described above, link width represents relative read abundance of

arthropod OTUs collected on each plant taxon (Alberdi et al., 2019); in other words, link width corresponds to the relative frequency of each association.

The information contained in ecological networks can be summarized in various ways. Qualitative properties used to describe networks, which treat all interactions as equal irrespective of their magnitude or frequency, tend to be highly sensitive to variation in sampling effort (Goldwasser & Roughgarden, 1997; Martinez et al., 1999). Quantitative metrics that weight each taxon by the total amount of its incoming and outgoing biomass flows (Bersier et al., 2002) are more robust to sampling differences (Banašek-Richter et al., 2004). Using the 'networklevel' commands in the R package bipartite (Dormann et al., 2008) we calculated six quantitative indices for our bipartite networks of arthropods and associated plants: (1) linkage density, (2) connectance, (3) generality, (4) vulnerability, (5) interaction evenness, and (6) the index of specialization H_2' (Table 2), that we reasoned would be associated with network specialization (Table 1). We converted each matrix to a binary presence-absence matrix and calculated the qualitative equivalent of: (1) linkage density, (2) connectance, (3) generality, and (4) vulnerability. We additionally calculated the ratio of resource species to consumers for the qualitative matrices, which is the ratio of plant genera to arthropod OTUs. These metrics represent the most fundamental biological and ecological properties of a community. We reasoned that the simplest metrics are a reasonable starting point given the limited understanding of how evolution shapes network structure, which would be necessary to justify the application of more involved network metrics. Further, these metrics have values that are interpretable with respect to their effect on specialization over time.

Tests of network metric significance and correlation between network properties

We used null models (Vázquez & Aizen, 2006) to test the statistical significance of empirical network metric values for the weighted data. For each weighted empirical network, we generated 1000 synthetic networks so that the total number of interactions and the identity of interaction partners is maintained while the weight associated with each interaction is shuffled (Staniczenko et al., 2013). With this simple quantitative null model, the distribution of interaction weights is conserved, along with the pattern of binary interactions, but not the identities of which interaction partners are associated with which weights. In terms of biological reasoning, the null model assumes that the identities of any two species

involved in a non-forbidden interaction are unimportant for explaining network metrics. We calculated p-values and z-scores for each combination of empirical network and metric by comparing the observed metric value calculated from the empirical network to the distribution of metric values calculated from synthetic matrices generated by the null model, i.e., the p-value quantifies how unlikely the observed, empirical metric value is to have been generated by the null model.

To compare the effect of community assembly on network size, arthropod diversity, and network metrics, we regressed the dependent variables by mean substrate age for each collection site. The untransformed substrate age data departed significantly from normality, so comparisons were performed using regressions on natural log-transformed substrate age data (Cowie, 1995; Gruner, 2007). We tested the significance of the correlation between network size and community age, each network metric and community age, and each network metric and network size, using Spearman's correlation tests. Additionally, we fit a second-degree polynomial equation for the curvilinear relationship between the index of specialization H_2' and community age.

Results

Composition of communities

Sites were selected using climatic and lidar data to restrict abiotic and biotic variation between sites so the effect of community age on ecological network structure could best be explored (SI Table 1 and SI Table 2). There was some variation in forest structure as would be expected with sites during primary succession (e.g., forest height and density changes) (SI Figure 2). Our ecological networks document 34 plant genera and 3517 arthropod OTUs, distributed across six classes: Entognatha, Crustacea (Amphipods and Isopods), Insecta, Arachnida, Chilopoda, and Diplopoda. The arthropod-plant associations in our networks represent many kinds of trophic and non-trophic biotic interactions that capture functional differences among species of the understory of the Hawaiian native forest. The barcode reference library increased taxonomic assignment from low taxonomic resolution to genus or species for 401 OTUs. Confident assignment was accomplished for a percentage of OTUs at each taxonomic level: Order 99.9%, Family 67.3%, Genus 38.1% and Species 24.9% (SI Table 3).

There were 2747 OTUs classified as native and 770 classified as non-native using NIClassify. The overall accuracy for our dataset predictions of nativeness using NIClassify was 99.9%. Of the native OTUs, Hemiptera were the dominant order (652 OTUs), followed by Araneae (467 OTUs), Diptera (327 OTUs), and Coleoptera (266 OTUs). We found a highly significant (SI Table 4) increase in network size with community age for both nodes and links, with a disproportionate increase in the number of links (interactions) after several hundred years of community development (Figure 2a). The number of native arthropod species increases dramatically over both ecological and evolutionary time while the number of non-native arthropod species remains relatively steady (Figure 2b). The abundance of native and non-native arthropods peaks in the middle-aged communities but the proportion of non-native taxon abundance is highest in younger communities (Figure 2c). Plant diversity increased with community age (Figure 2d).

Arthropod-plant association networks

Arthropod OTU richness, plant diversity and number of interactions increased with the geologic age of the site. Bipartite networks of younger communities contain linkage widths between the few dominant taxa (e.g., Hemiptera and *Metrosideros*) while older communities contain smaller linkage widths representative of the many more associations distributed among the greater diversity of both higher and lower level taxa (Figure 3, SI Figure 3).

For the null model analyses of the weighted matrices, some observed network metric values were not significantly different ($p<0.05$) from metric values produced from the synthetic matrices (SI Table 5, SI Figure 6).

Results of the Spearman's correlation tests show linkage density (average number of interactions per species), network vulnerability (a measure of the ratio of plant generic richness to arthropod OTU richness) and interaction evenness (a measure of the uniformity of energy flows along different pathways) increased significantly with community age (Figure 4, Table 3). Generality (a measure of the ratio of

arthropod OTU richness to plant generic richness) and the index of specialization H_2' both increased with community age but were not significantly positively correlated. The index of specialization H2' has a curvilinear relationship with community age, first decreasing then increasing. A second-degree polynomial provides the best approximation of the relationship between the H_2' and community age ($F = 6.85$, $R^2 = 0.5392$, $p < 0.05$). By beat sampling and sequencing all plant-associated arthropods, our sampling of arthropod taxa is at finer taxonomic resolution than plants. As a result, generality (links/arthropods) is very close arithmetically to linkage density (links/arthropods + plants) in our dataset because the number of arthropod OTUs is many times greater than the number of plant genera for all communities. Connectance (proportion of realized interactions) was not significantly correlated with increasing community age, but instead is highest at the youngest site, and relatively constant for the remainder of sites.

For the qualitative metrics calculated from the binary matrices, linkage density (links/species), connectance links/(arthropods*plants), and generality (links/arthropods) were significantly correlated with community age, while vulnerability (links/plants) and the ratio of resource species to consumers (plants/arthropods) was not (SI Figure 4, SI Table 4). The results from plot level analysis are consistent with the site level data and the variance among plots at the same sites is minimal (SI Figure 7). These results help corroborate the trend of increasing specialization over time.

For the regressions of network metrics against network size, with the exception of generality, quantitative network metrics were not significantly correlated with network size (SI Figure 5A, SI Table 4). By contrast, qualitative metrics were significantly correlated with network size with the exception of the ratio of resource species to consumers, and vulnerability (SI Figure 5B, SI Table 4).

Discussion

Using a dataset of biotic associations during the course of community assembly here we present strong evidence of increasing specialization within arthropod communities through evolutionary time. Our DNA metabarcoding data have allowed us to collect a large sample of the arthropods from the understory of Hawaiian forests, representing a broad swath of trophic and non-trophic arthropod-plant associations. As

456 expected, the qualitative metrics were strongly biased by network size (Banašek-Richter et al., 2004;
457 Goldwasser & Roughgarden, 1997) and showed higher linkage density, generality, vulnerability,
458 interaction evenness, and lower connectance in older communities, because the diversity of plants and
459 arthropods was higher in these communities (SI Figure 4, SI Table 4). Our null model analysis helped to
460 demonstrate that the distribution of link weights was itself an important feature of the observed network
461 structure (i.e., not which species they are between). We present clear signatures of change in
462 quantitative, weighted network metrics with community age (Figure 4, Table 3) that resulted from
463 changing community composition and ecological dynamics.
464
465 *Ecological processes dominate younger communities*
466
467 Theory suggests that the composition of the youngest communities is shaped through colonization from a
468 regional species pool. This expectation is supported by our results, with the younger communities having
469 significantly lower linkage density, vulnerability, and interaction evenness (Figure 4). These results
470 indicate that species in younger communities are interacting with greater frequency along less uniform
471 interaction pathways, compared to species assemblages at older sites. However, notably the very
472 youngest site, the 1973 lava flow, is an outlier. At the 1973 lava flow, linkage density is high (*LD* = 24.2),
473 likely reflecting strong environmental filtering and an opportunistic community of generalist species
474 (Bufford et al., 2020; Kortsch et al., 2015) suited for survival during primary succession. At other young
475 sites, linkage density is low, from < 10 (Tree Planting Rd.) whereas it peaks and levels off at Maui (*LD* =
476 38.6) and Kauai (*LD* = 38.9), respectively. Thus, linkage density was low at young sites with low resource
477 diversity while the diversity of interactions increased over evolutionary time in step with increasing
478 community complexity.
479
480 Interaction evenness was low, as expected, on the youngest sites, again with the exception of the 1973
481 flow. As a measure of the uniformity of energy flows along different pathways, we expected interaction
482 evenness to be low in young communities because some interaction partners would dominate the
483 associations in the network. For example, a large proportion of interactions on the youngest sites (< 300

484 years old) belong to the associations of Hemiptera and Collembola species with early successional plant
485 species, *Metrosideros polymorpha* and *Dicranopteris linearis* (Figure 3, SI Figure 3). Low interaction
486 evenness has also been demonstrated among bees and wasps and their associated natural enemies
487 (e.g. parasitoids) under conditions of intensive management (Staniczenko et al., 2017; Tylianakis et al.,
488 2007). The early successional communities in Hawaii are ecologically similar to highly modified sites, due
489 to the recent disturbance from lava and the paucity of resource diversity. We suggest that the higher
490 interaction evenness at the 1973 lava flow is due to the extremely limited resources (plants) on the
491 sparsely vegetated lava substrate. At this site colonists may be joined by a relatively large representation
492 of transient arthropods, which may be less host-specific and appear randomly associated with the
493 available plants, increasing interaction evenness. Connectance also peaked in the youngest community
494 (1973 lava flow) likely due to the greater representation of generalists within this network (Kortsch et al.,
495 2015; Ponisio et al., 2019).
496
497 The network metric values are less consistent among the youngest sites compared to the older sites
498 (Figure 4). This is likely due to the relatively rapid changes in community composition in early primary
499 succession (Atkinson, 1970; Roderick et al., 2012) compared to older established sites. An alternative
500 explanation is that change in the composition of the understory plants (Figure 3 and SI Figure 3) and
501 canopy structure (SI Figure 2 and SI Table 2) results in the network metric variation at the youngest sites.
502 The higher variation among network values at the youngest sites may also point to the different rates of
503 specialization and adaptation among different lineages of arthropods. Among functional groups of beetles
504 (e.g., xylophages, fungivores, predators), community composition and network specialization changed
505 differently during early succession (Wende et al., 2017).
506
507 *Specialization increases through evolutionary time*
508
509 For a given taxon on average, the number of biotic interactions it is involved in decreases with community
510 age, resulting in greater network specialization. This is reflected in the increased linkage density with
511 community age, as early colonizing species gave way to a greater diversity of associations (Figure 4).

512 However, weighted connectance stabilized at around the same level for the remainder of the communities
513 after the 1973 lava flow. This may be explained by the 'constant connectance' hypothesis (Martinez,
514 1992) that posits that species are linked to a fixed fraction of species in a network, independent of the
515 number of species in a community. A similar pattern of constant connectance and community age was
516 found in arthropods recolonizing defaunated mangrove islands (Piechnik et al., 2008). For the Hawaiian
517 Islands, several factors likely produce constant connectance over long-term community development.
518 First, resource availability limits specialists at early stages; e.g., Escape Road (~ 300 yrs) is dominated by
519 a single species of fern. Next, over evolutionary time, the Hawaiian fauna is characterized by a
520 remarkably high rate of lineage diversification (Gillespie, 2016; Gillespie et al., 2020; Zimmerman, 1970)
521 that has added novel species and associations. Finally, at more recent timescales (after human arrival)
522 immigration of non-natives has been sufficiently high so as to add generalist taxa across all stages of
523 community development (Figure 2b).
524
525 A previous study which used an island chronosequence to examine how pollinator interactions change
526 through extended time (Trøjelsgaard et al 2013) also found connectance was poorly explained by age.
527 However, contrary to our results, the Canary Islands study showed hump-shaped relationships of
528 interaction richness and specialization with island age. One reason for the different results is that we used
529 a natural log scale for the skewness of island age. For the Hawaiian islands, values for linkage density,
530 vulnerability, interaction evenness, and index of specialization H_2' were especially high on the volcano of
531 East Maui. The islands of Maui Nui are also where richness peaks for many native arthropod lineages
532 (Gillespie & Baldwin, 2009; Gruner, 2007). However, unlike the Canary Island pollinators, our values of
533 linkage density were highest on the oldest island, and values for interaction evenness, vulnerability, and
534 index of specialization H_2' were nearly as high, indicating that the overall changes in network structure
535 were more linear than hump-shaped. An alternative explanation for the difference in the results is that the
536 older islands of the Canary archipelago have environments that are very different from the younger
537 islands. Although the Canary Island study focused on communities that were characterized by the plant
538 species *Euphorbia balsamifera*, the abiotic environment changes significantly across their
539 chronosequence, with the older islands much lower and drier (Juan et al., 2000). Thus, the finding of a

hump-shaped relationship in the Canary Islands is associated with the combined effects of time, island geomorphological transitions, and associated change in climate regimes. In contrast, the current study in the Hawaiian Islands aimed to standardize environments (elevation, precipitation, and forest cover, with sampling from standardized plots across the islands). Therefore, any confounding environmental differences were minimized and changes in network properties should largely reflect the influence of community age.

Vulnerability and generality both show positive correlations with community age (Figure 4, Table 3), thus the average number of arthropods per plant species (vulnerability) and the average number of plant species per arthropod (generality) are increasing over time. This is consistent with our expectation that specialization increases resource overlap when a reduction in antagonistic interactions leads to some level of resource redundancy and an increase in diversity of beneficial interactions leads to greater resource complementarity (Table 1). In other words, over evolutionary time, if two species are in direct competition for resources, they can evolve traits that allow them to coexist. One result of trait matching between interaction partners is decreasing niche breadth (i.e., decreasing diversity of resources used). Thus, our results are consistent with decreasing niche breadth with island age found previously from literature for herbivores (Ponisio et al., 2019). Moreover, although the rate of specialization and adaptation, such as occurs through trait matching and decreasing niche breadth, can vary among functional groups in a community, our data show that community specialization is happening at the network level, averaging over the high variation in rates of specialization.

The network-level specialization index H2' is largely unaffected by network size, network architecture or total number of interactions for a fixed matrix size (Blüthgen et al. 2006), making it an ideal metric compare between different networks for understanding specialization over time. We find that the index of specialization increases over time but is better fit by a second-degree polynomial equation. In early stage communities from 50 to 575 years the index of specialization is decreasing. This drop in specialization in the first several hundred years, is followed by an increase over the next tens of thousands of years. For random associations H_2' is usually close to zero. On Maui it reaches a value of 0.6 then levels out to 0.5

568 on Molokai and Kauai. This pattern is consistent with other metrics in our analysis suggesting that very
569 young communities are organized by assembly rules making them appear specialized. After ecological
570 sorting and the impact of *in situ* evolution in later stage communities we see organization at a secondary,
571 evolutionary stage of development.
572
573 *Resilience of communities increases through time*
574
575 While communities sampled from the youngest sites are composed primarily of native species from the
576 regional pool (Figure 2b), younger communities have proportionally higher abundances of non-native
577 species infiltrating the system (Figure 2c). Thus, it appears that young communities are more invasible,
578 which is consistent with previous studies showing that communities composed of endemic generalist taxa
579 are more vulnerable to infiltration by non-natives (Olesen et al., 2002). By increasing connectance and
580 lowering network specialization, higher numbers of alien species may in turn facilitate increasing numbers
581 and impacts of invasions (Simberloff, 2006; Simberloff & Von Holle, 1999).
582
583 However, this result runs counter to work suggesting higher-connectance food webs tend to host fewer
584 invaders and exert stronger biotic resistance compared to low-connectance webs (Smith-Ramesh et al.,
585 2017). Further, community resistance to invasion is known to increase with native species diversity
586 (Gallien & Carboni, 2017) and network complexity (Wei et al., 2015). Considering the results from our
587 study within the context of this previous work, older communities, which are characterized by low
588 connectance and high specialization, may be more resistant to invasion; however, individual taxa may be
589 more susceptible to extinction. From an individual species level, because all species are linked together
590 either directly or indirectly (Montoya et al., 2006), individual species with high specialization and low
591 connectance are susceptible to extinction because of secondary extinctions occurring when specialized
592 consumers lose their only prey (Dunne et al., 2002; Staniczenko et al., 2010). From a network level, as
593 communities age, several species may be associated with the same resource (resource redundancy) or
594 utilize a single resource more effectively (resource complementarity), minimizing variability in the

595 functioning of an ecosystem, for example when some consumer species decline in number (Peralta et al.,
596 2014).
597
598 Although ecological processes, such as interspecific interactions or disturbance, are often attributed to
599 the geographical differences in exotic species richness (Lockwood et al., 2013) an alternative explanation
600 for the apparent reduced biotic resistance to invasion of younger communities may be that they
601 experience increased propagule pressure (Lockwood et al., 2005). The younger sites on Kilauea volcano
602 are accessed more frequently by tourists compared to the older sites, which require greater on foot
603 distances to reach or special access permits. Furthermore, while our study directly assesses arthropod-
604 plant associations, it only indirectly measures the effect of higher trophic associations. Differential top-
605 down pressure (e.g., predator turnover) during community assembly likely also changes biotic resistance
606 to invasion, for example, generalist insectivorous birds reduced infiltration of an invasive species of spider
607 at the 133 years old Tree Planting Rd. community (Gruner, 2005).
608
609 *Conclusions and outlook*
610
611 Our study uses whole-community DNA metabarcoding data to assess the biotic associations of
612 thousands of arthropod OTUs on plants across a geological chronosequence. By including relative
613 abundance data, we achieve a signature of interaction strength (Popovic et al., 2019) not captured for co-
614 occurrences with presence-absence observations (Blanchet et al., 2020). Although DNA metabarcoding
615 can be used for observation of trophic interactions (Alberdi et al., 2019; Krehenwinkel, Kennedy, et al.,
616 2017), our analysis instead includes all biotic associations between arthropod-plant communities,
617 including those that can be difficult to detect (e.g. involving cryptic species, new non-natives, endangered
618 species, juveniles). Thus, we are able to include complex community interactions including substrates
619 chosen for acoustic signaling (Mullet et al., 2017), predator avoidance (Lindstedt et al., 2019; Stachowicz
620 & Hay, 1999) and gregarious plant-feeding insects (Hunter, 2000) that are often overlooked in traditional
621 network studies. Compared to the limitations of small, unweighted early food web studies (Cohen et al.,

1993; Hall & Raffaelli, 1991) DNA metabarcoding offers exciting avenues forward for capturing community complexity.

This research revealed a strong association between the network structure of ecological communities and community development over evolutionary time. Quantitative network metrics demonstrate that younger communities are composed of more generalist species that interact with greater frequency along fewer interaction pathways, with individual and network specialization increasing with community age. Our data highlight the utility of DNA metabarcoding for understanding longstanding questions of ecology and evolutionary biology that remain time consuming (e.g., keying out morphological species) or impossible (e.g., identification of juveniles) to assess with traditional methods. From a conservation perspective, our results indicate that habitat disturbance erodes a complex web of biotic associations, far greater than the sum of the community metrics of richness and abundance, that have evolved *in situ* over thousands to millions of years.

Acknowledgements

We would like to thank the field collection team including Curtis Ewing, Andy Rominger, Elske Tielens, Thomas Fezza, Kylle Roy, Christa Nicols, Madeline Stark, Brendan Cote, Kalena Shiroma, Loreto Villegas-Villeza, and Monica Sheffer as well as the many undergraduate students at UH Hilo and UC Berkeley that helped to identify arthropod specimens and sort them to size. Airborne laser scanning data collection and processing was provided by Greg Asner of Arizona State University's Global Airborne Observatory. The GAO is made possible by support from private foundations, visionary individuals, and Arizona State University. We are indebted to many scientists and land managers in Hawaii who have provided access to the lands: Pat Bily (The Nature Conservancy of Hawaii), Melissa Dean, Christian Giardina, and Tabetha Block (Hawaii Experimental Tropical Forests), the late Betsy Gagne (Natural Area Reserve System), Lisa Hadway, Steve Bergfeld, and Joey Mello (Department of Forestry and Wildlife Hilo), Cynthia King and Charmian Dang (Department of Land and Natural Resources) and Rhonda Loh (Hawaii Volcanoes National Park). N.R.G. was supported by the Robert van den Bosch Memorial

650 Scholarship and Philomathia Environmental Science Fellowship. The research was supported by an NSF
651 Dimensions in Biodiversity grant to R.G.G. (DEB 1241253) and D.S.G. (DEB-1240774).

652

653 **References**

654 Aizen, M. A., Morales, C. L., & Morales, J. M. (2008). Invasive mutualists erode native pollination webs.
655 *PLoS Biology*, *6*(2), e31.
656 Alberdi, A., Aizpurua, O., Bohmann, K., Gopalakrishnan, S., Lynggaard, C., Nielsen, M., & Gilbert, M. T. P.
657 (2019). Promises and pitfalls of using high-throughput sequencing for diet analysis. *Molecular*
658 *Ecology Resources*, *19*(2), 327–348. https://doi.org/10.1111/1755-0998.12960
659 Andersen, J. C., Oboyski, P., Davies, N., Charlat, S., Ewing, C., Meyer, C., Krehenwinkel, H., Lim, J. Y.,
660 Noriyuki, S., Ramage, T., Gillespie, R. G., & Roderick, G. K. (2019). Categorization of species as
661 native or nonnative using DNA sequence signatures without a complete reference library.
662 *Ecological Applications*, *29*(5), e01914. https://doi.org/10.1002/eap.1914
663 Andujar, C., Creedy, T. J., Arribas, P., López, H., Salces-Castellano, A., Pérez-Delgado, A. J., Vogler, A. P., &
664 Emerson, B. C. (2021). Validated removal of nuclear pseudogenes and sequencing artefacts from
665 mitochondrial metabarcode data. *Molecular Ecology Resources*, *21*(6), 1772–1787.
666 Asner, G. P., Hughes, R. F., Vitousek, P. M., Knapp, D. E., Kennedy-Bowdoin, T., Boardman, J., Martin, R.
667 E., Eastwood, M., & Green, R. O. (2008). Invasive plants transform the three-dimensional
668 structure of rain forests. *Proceedings of the National Academy of Sciences*, *105*(11), 4519–4523.
669 https://doi.org/10.1073/pnas.0710811105
670 Asner, G. P., Knapp, D. E., Boardman, J., Green, R. O., Kennedy-Bowdoin, T., Eastwood, M., Martin, R. E.,
671 Anderson, C., & Field, C. B. (2012). Carnegie Airborne Observatory-2: Increasing science data
672 dimensionality via high-fidelity multi-sensor fusion. *Remote Sensing of Environment*, *124*, 454–
673 465.
674 Asner, G. P., Knapp, D. E., Kennedy-Bowdoin, T., Jones, M. O., Martin, R. E., Boardman, J. W., & Field, C.
675 B. (2007). Carnegie Airborne Observatory: In-flight fusion of hyperspectral imaging and
676 waveform light detection and ranging for three-dimensional studies of ecosystems. *Journal of*
677 *Applied Remote Sensing*, *1*(1), 013536. https://doi.org/10.1117/1.2794018
678 Atkinson, A. E. (1970). Successional Trends in the Coastal and Lowland Forest of Mauna Loa and Kilauea
679 Volcanoes, Hawaii! *PACIFIC SCIENCE*, *24*, 14.
680 Bálint, M., Pfenninger, M., Grossart, H.-P., Taberlet, P., Vellend, M., Leibold, M. A., Englund, G., &
681 Bowler, D. (2018). Environmental DNA time series in ecology. *Trends in Ecology & Evolution*,
682 *33*(12), 945–957.
683 Banašek-Richter, C., Cattin, M.-F., & Bersier, L.-F. (2004). Sampling effects and the robustness of
684 quantitative and qualitative food-web descriptors. *Journal of Theoretical Biology*, *226*(1), 23–32.
685 https://doi.org/10.1016/S0022-5193(03)00305-9
686 Bersier, L.-F., Banašek-Richter, C., & Cattin, M.-F. (2002). Quantitative Descriptors of Food-Web
687 Matrices. *Ecology*, *83*(9), 2394–2407.
688 Blanchet, F. G., Cazelles, K., & Gravel, D. (2020). Co-occurrence is not evidence of ecological interactions.
689 *Ecology Letters*, *23*(7), 1050–1063.
690 Blüthgen, N., Menzel, F. & Blüthgen, N. (2006). Measuring specialization in species interaction networks.
691 BMC Ecol 6, 9. https://doi.org/10.1186/1472-6785-6-9

692 Bohan, D. A., Caron-Lormier, G., Muggleton, S., Raybould, A., & Tamaddoni-Nezhad, A. (2011).
693 Automated discovery of food webs from ecological data using logic-based machine learning.
694 *PLoS One*, *6*(12), e29028.
695 Boon, E., Meehan, C. J., Whidden, C., Wong, D. H.-J., Langille, M. G., & Beiko, R. G. (2014). Interactions in
696 the microbiome: Communities of organisms and communities of genes. *FEMS Microbiology*
697 *Reviews*, *38*(1), 90–118.
698 Brodie, J. F. (2017). Evolutionary cascades induced by large frugivores. *Proceedings of the National*
699 *Academy of Sciences*, *114*(45), 11998–12002.
700 Bufford, J. L., Hulme, P. E., Sikes, B. A., Cooper, J. A., Johnston, P. R., & Duncan, R. P. (2020). Novel
701 interactions between alien pathogens and native plants increase plant–pathogen network
702 connectance and decrease specialization. *Journal of Ecology*, *108*(2), 750–760.
703 Castro-Urgal, R., & Traveset, A. (2014). Differences in flower visitation networks between an oceanic and
704 a continental island. *Botanical Journal of the Linnean Society*, *174*(3), 478–488.
705 https://doi.org/10.1111/boj.12134
706 Chamberlain, S. A., Cartar, R. V., Worley, A. C., Semmler, S. J., Gielens, G., Elwell, S., Evans, M. E., Vamosi,
707 J. C., & Elle, E. (2014). Traits and phylogenetic history contribute to network structure across
708 Canadian plant–pollinator communities. *Oecologia*, *176*(2), 545–556.
709 Clague, D. A. (1996). The growth and subsidence of the Hawaiian-Emperor volcanic chain. *The Origin and*
710 *Evolution of Pacific Island Biotas, New Guinea to Eastern Polynesia: Patterns and Processes*, 35–
711 50.
712 Clare, E. L. (2014). Molecular detection of trophic interactions: Emerging trends, distinct advantages,
713 significant considerations and conservation applications. *Evolutionary Applications*, *7*(9), 1144–
714 1157.
715 Cohen, J. E., Beaver, R. A., Cousins, S. H., DeAngelis, D. L., Goldwasser, L., Heong, K. L., Holt, R. D., Kohn,
716 A. J., Lawton, J. H., & Martinez, N. (1993). Improving food webs. *Ecology*, *74*(1), 252–258.
717 Coux, C., Rader, R., Bartomeus, I., & Tylianakis, J. M. (2016). Linking species functional roles to their
718 network roles. *Ecology Letters*, *19*(7), 762–770. https://doi.org/10.1111/ele.12612
719 Cowie, R. H. (1995). Variation in Species Diversity and Shell Shape in Hawaiian Land Snails: In Situ
720 Speciation and Ecological Relationships. *Evolution*, *49*(6), 1191–1202.
721 https://doi.org/10.1111/j.1558-5646.1995.tb04446.x
722 de Kerdrel, G. A., Andersen, J. C., Kennedy, S. R., Gillespie, R., & Krehenwinkel, H. (2020). Rapid and cost-
723 effective generation of single specimen multilocus barcoding data from whole arthropod
724 communities by multiple levels of multiplexing. *Scientific Reports*, *10*(1), 1–12.
725 Dell, J. E., Salcido, D. M., Lumpkin, W., Richards, L. A., Pokswinski, S. M., Loudermilk, E. L., O'Brien, J. J., &
726 Dyer, L. A. (2019). Interaction diversity maintains resiliency in a frequently disturbed ecosystem.
727 *Frontiers in Ecology and Evolution*, *7*, 145.
728 Delmas, E., Besson, M., Brice, M.-H., Burkle, L. A., Dalla Riva, G. V., Fortin, M.-J., Gravel, D., Guimarães
729 Jr., P. R., Hembry, D. H., Newman, E. A., Olesen, J. M., Pires, M. M., Yeakel, J. D., & Poisot, T.
730 (2019). Analysing ecological networks of species interactions. *Biological Reviews*, *94*(1), 16–36.
731 https://doi.org/10.1111/brv.12433
732 Dormann, C. F., Gruber, B., & Fründ, J. (2008). Introducing the bipartite package: Analysing ecological
733 networks. *Interaction*, *1*(0.2413793).
734 Dunne, J. A., & Williams, R. J. (2009). Cascading extinctions and community collapse in model food webs.
735 *Philosophical Transactions of the Royal Society B: Biological Sciences*, *364*(1524), 1711–1723.
736 Dunne, J. A., Williams, R. J., & Martinez, N. D. (2002). Network structure and biodiversity loss in food
737 webs: Robustness increases with connectance. *Ecology Letters*, *5*(4), 558–567.
738 Edgar, R. C. (2010). Search and clustering orders of magnitude faster than BLAST. *Bioinformatics*, *26*(19),
739 2460–2461.

740 Edgar, R. C. (2016). UNOISE2: Improved error-correction for Illumina 16S and ITS amplicon sequencing.
741 *BioRxiv*, 081257.
742 Elbrecht, V., & Leese, F. (2015). Can DNA-based ecosystem assessments quantify species abundance?
743 Testing primer bias and biomass—sequence relationships with an innovative metabarcoding
744 protocol. *PloS One*, *10*(7), e0130324.
745 Faust, K., & Raes, J. (2012). Microbial interactions: From networks to models. *Nature Reviews*
746 *Microbiology*, *10*(8), 538–550. https://doi.org/10.1038/nrmicro2832
747 Fricke, E. C., Tewksbury, J. J., Wandrag, E. M., & Rogers, H. S. (2017). Mutualistic strategies minimize
748 coextinction in plant–disperser networks. *Proceedings of the Royal Society B: Biological Sciences*,
749 *284*(1854), 20162302. https://doi.org/10.1098/rspb.2016.2302
750 Gagne, W. C., & Cuddihy, L. W. (1990). *Vegetation. Manual of the flowering plants of Hawaii*. University
751 of Hawaii Press, Honolulu.
752 Gallien, L., & Carboni, M. (2017). The community ecology of invasive species: Where are we and what's
753 next? *Ecography*, *40*(2), 335–352. https://doi.org/10.1111/ecog.02446
754 *Gap Analysis Project | U.S. Geological Survey*. (2019, July 29). https://www.usgs.gov/programs/gap-
755 analysis-project
756 Giambelluca, T. W., Chen, Q., Frazier, A. G., Price, J. P., Chen, Y.-L., Chu, P.-S., Eischeid, J. K., & Delparte,
757 D. M. (2013). Online rainfall atlas of Hawai 'i. *Bulletin of the American Meteorological Society*,
758 *94*(3), 313–316.
759 Gibson, J., Shokralla, S., Porter, T. M., King, I., Konynenburg, S. van, Janzen, D. H., Hallwachs, W., &
760 Hajibabaei, M. (2014). Simultaneous assessment of the macrobiome and microbiome in a bulk
761 sample of tropical arthropods through DNA metasystematics. *Proceedings of the National*
762 *Academy of Sciences*, *111*(22), 8007–8012. https://doi.org/10.1073/pnas.1406468111
763 Gillespie. (2016). Island time and the interplay between ecology and evolution in species diversification.
764 *Evolutionary Applications*, *9*(1), 53–73. https://doi.org/10.1111/eva.12302
765 Gillespie, R. G., & Baldwin, B. G. (2009). Island biogeography of remote archipelagoes. In J. B. Losos & R.
766 E. Ricklefs (Eds.), *The Theory of Island Biogeography Revisited* (pp. 358–387). Princeton
767 University Press.
768 Gillespie, R. G., Bennett, G. M., De Meester, L., Feder, J. L., Fleischer, R. C., Harmon, L. J., Hendry, A. P.,
769 Knope, M. L., Mallet, J., & Martin, C. (2020). Comparing adaptive radiations across space, time,
770 and taxa. *Journal of Heredity*, *111*(1), 1–20.
771 Goldwasser, L., & Roughgarden, J. (1997). Sampling Effects and the Estimation of Food-Web Properties.
772 *Ecology*, *78*(1), 41–54. https://doi.org/10.1890/0012-9658(1997)078[0041:SEATEO]2.0.CO;2
773 Gordon, A., & Hannon, G. J. (2010). Fastx-toolkit. *FASTQ/A Short-Reads Preprocessing Tools*
774 *(Unpublished) Http://Hannonlab. Cshl. Edu/Fastx_toolkit*, *5*.
775 Graham, N. R., Gillespie, R. G., & Krehenwinkel, H. (2021). Towards Eradicating the Nuisance of Numts
776 and Noise in Molecular Biodiversity Assessment. *Molecular Ecology Resources*, *n/a*(n/a).
777 https://doi.org/10.1111/1755-0998.13414
778 Gruner, D. S. (2005). Biotic resistance to an invasive spider conferred by generalist insectivorous birds on
779 Hawai'i Island. *Biological Invasions*, *7*(3), 541–546. https://doi.org/10.1007/s10530-004-2509-2
780 Gruner, D. S. (2007). Geological age, ecosystem development, and local resource constraints on
781 arthropod community structure in the Hawaiian Islands. *Biological Journal of the Linnean*
782 *Society*, *90*(3), 551–570.
783 Hall, S. J., & Raffaelli, D. (1991). Food-web patterns: Lessons from a species-rich web. *The Journal of*
784 *Animal Ecology*, 823–841.
785 Hembry, D. H., Raimundo, R. L., Newman, E. A., Atkinson, L., Guo, C., Guimarães Jr, P. R., & Gillespie, R.
786 G. (2018). Does biological intimacy shape ecological network structure? A test using a brood

787 pollination mutualism on continental and oceanic islands. *Journal of Animal Ecology*, *87*(4),
788 1160–1171.
789 Hrček, J., & Godfray, H. C. J. (2015). What do molecular methods bring to host–parasitoid food webs?
790 *Trends in Parasitology*, *31*(1), 30–35.
791 Hubbell, S. P. (2001). *The Unified Neutral Theory of Species Abundance and Diversity*. Princeton
792 University Press.
793 Hunter, A. F. (2000). Gregariousness and repellent defences in the survival of phytophagous insects.
794 *Oikos*, *91*(2), 213–224. https://doi.org/10.1034/j.1600-0706.2000.910202.x
795 Juan, C., Emerson, B. C., Oromí, P., & Hewitt, G. M. (2000). Colonization and diversification: Towards a
796 phylogeographic synthesis for the Canary Islands. *Trends in Ecology & Evolution*, *15*(3), 104–109.
797 Kortsch, S., Primicerio, R., Fossheim, M., Dolgov, A. V., & Aschan, M. (2015). Climate change alters the
798 structure of arctic marine food webs due to poleward shifts of boreal generalists. *Proceedings of*
799 *the Royal Society B: Biological Sciences*, *282*(1814), 20151546.
800 https://doi.org/10.1098/rspb.2015.1546
801 Koskella, B., & Brockhurst, M. A. (2014). Bacteria–phage coevolution as a driver of ecological and
802 evolutionary processes in microbial communities. *FEMS Microbiology Reviews*, *38*(5), 916–931.
803 Koskella, B., Hall, L. J., & Metcalf, C. J. E. (2017). The microbiome beyond the horizon of ecological and
804 evolutionary theory. *Nature Ecology & Evolution*, *1*(11), 1606–1615.
805 Krehenwinkel, H., Kennedy, S., Pekár, S., & Gillespie, R. G. (2017). A cost-efficient and simple protocol to
806 enrich prey DNA from extractions of predatory arthropods for large-scale gut content analysis by
807 Illumina sequencing. *Methods in Ecology and Evolution*, *8*(1), 126–134.
808 Krehenwinkel, H., Wolf, M., Lim, J. Y., Rominger, A. J., Simison, W. B., & Gillespie, R. G. (2017). Estimating
809 and mitigating amplification bias in qualitative and quantitative arthropod metabarcoding.
810 *Scientific Reports*, *7*(1), 1–12.
811 Lange, V., Böhme, I., Hofmann, J., Lang, K., Sauter, J., Schöne, B., Paul, P., Albrecht, V., Andreas, J. M., &
812 Baier, D. M. (2014). Cost-efficient high-throughput HLA typing by MiSeq amplicon sequencing.
813 *BMC Genomics*, *15*(1), 1–11.
814 Lim, J. Y., Patiño, J., Noriyuki, S., Cayetano, L., Gillespie, R. G., & Krehenwinkel, H. (2021). Semi-
815 quantitative metabarcoding reveals how climate shapes arthropod community assembly along
816 elevation gradients on Hawaii Island. *Molecular Ecology*.
817 Lindstedt, C., Murphy, L., & Mappes, J. (2019). Antipredator strategies of pupae: How to avoid predation
818 in an immobile life stage? *Philosophical Transactions of the Royal Society B*, *374*(1783),
819 20190069.
820 Lockwood, J. L., Cassey, P., & Blackburn, T. (2005). The role of propagule pressure in explaining species
821 invasions. *Trends in Ecology & Evolution*, *20*(5), 223–228.
822 https://doi.org/10.1016/j.tree.2005.02.004
823 Lockwood, J. L., Hoopes, M. F., & Marchetti, M. P. (2013). *Invasion Ecology*. John Wiley & Sons.
824 Martinez, N. D., Hawkins, B. A., Dawah, H. A., & Feifarek, B. P. (1999). Effects of Sampling Effort on
825 Characterization of Food-Web Structure. *Ecology*, *80*(3), 1044–1055.
826 Mata, V. A., da Silva, L. P., Veríssimo, J., Horta, P., Raposeira, H., McCracken, G. F., Rebelo, H., & Beja, P.
827 (2021). Combining DNA metabarcoding and ecological networks to inform conservation
828 biocontrol by small vertebrate predators. *Ecological Applications*, *31*(8), e02457.
829 McGill, B. J., Chase, J. M., Hortal, J., Overcast, I., Rominger, A. J., Rosindell, J., Borges, P. A. V., Emerson,
830 B. C., Etienne, R. S., Hickerson, M. J., Mahler, D. L., Massol, F., McGaughran, A., Neves, P.,
831 Parent, C., Patiño, J., Ruffley, M., Wagner, C. E., & Gillespie, R. (2019). Unifying macroecology
832 and macroevolution to answer fundamental questions about biodiversity. *Global Ecology and*
833 *Biogeography*, *28*(12), 1925–1936. https://doi.org/10.1111/geb.13020

834 Miller, Pfeiffer, W., & Schwartz, T. (2010). Creating the CIPRES Science Gateway for inference of large
835 phylogenetic trees. *2010 Gateway Computing Environments Workshop (GCE)*, 1–8.
836 https://doi.org/10.1109/GCE.2010.5676129
837 Montoya, J. M., Pimm, S. L., & Solé, R. V. (2006). Ecological networks and their fragility. *Nature*,
838 *442*(7100), 259–264.
839 Morella, N. M., Weng, F. C.-H., Joubert, P. M., Metcalf, C. J. E., Lindow, S., & Koskella, B. (2020).
840 Successive passaging of a plant-associated microbiome reveals robust habitat and host
841 genotype-dependent selection. *Proceedings of the National Academy of Sciences*, *117*(2), 1148–
842 1159.
843 Mullet, T. C., Farina, A., & Gage, S. H. (2017). The Acoustic Habitat Hypothesis: An Ecoacoustics
844 Perspective on Species Habitat Selection. *Biosemiotics*, *10*(3), 319–336.
845 https://doi.org/10.1007/s12304-017-9288-5
846 Münkemüller, T., Gallien, L., Pollock, L. J., Barros, C., Carboni, M., Chalmandrier, L., Mazel, F., Mokany,
847 K., Roquet, C., & Smyčka, J. (2020). Dos and don'ts when inferring assembly rules from diversity
848 patterns. *Global Ecology and Biogeography*, *29*(7), 1212–1229.
849 Newman, M. E. J., & Girvan, M. (2004). Finding and evaluating community structure in networks.
850 *Physical Review E*, *69*(2), 026113. https://doi.org/10.1103/PhysRevE.69.026113
851 Oksanen, J., Kindt, R., Legendre, P., O'Hara, B., Stevens, M. H. H., Oksanen, M. J., & Suggests, M. (2007).
852 The vegan package. *Community Ecology Package*, *10*(631–637), 719.
853 Olesen, J. M., Eskildsen, L. I., & Venkatasamy, S. (2002). Invasion of pollination networks on oceanic
854 islands: Importance of invader complexes and endemic super generalists. *Diversity and*
855 *Distributions*, *8*(3), 181–192.
856 Peralta, A. M., Sánchez, A. M., Luzuriaga, A. L., de Bello, F., & Escudero, A. (2019). Evidence of functional
857 species sorting by rainfall and biotic interactions: A community monolith experimental
858 approach. *Journal of Ecology*, *107*(6), 2772–2788.
859 Peralta, Frost, C. M., Rand, T. A., Didham, R. K., & Tylianakis, J. M. (2014). Complementarity and
860 redundancy of interactions enhance attack rates and spatial stability in host–parasitoid food
861 webs. *Ecology*, *95*(7), 1888–1896.
862 Piechnik, D. A., Lawler, S. P., & Martinez, N. D. (2008). Food-web assembly during a classic biogeographic
863 study: Species'"trophic breadth" corresponds to colonization order. *Oikos*, *117*(5), 665–674.
864 https://doi.org/10.1111/j.0030-1299.2008.15915.x
865 Poisot, T., Stouffer, D. B., & Gravel, D. (2015). Beyond species: Why ecological interaction networks vary
866 through space and time. *Oikos*, *124*(3), 243–251. https://doi.org/10.1111/oik.01719
867 Ponisio, L. C., Valdovinos, F. S., Allhoff, K. T., Gaiarsa, M. P., Barner, A., Guimarães Jr, P. R., Hembry, D.
868 H., Morrison, B., & Gillespie, R. (2019). A network perspective for community assembly.
869 *Frontiers in Ecology and Evolution*, *7*, 103.
870 Popovic, G. C., Warton, D. I., Thomson, F. J., Hui, F. K., & Moles, A. T. (2019). Untangling direct species
871 associations from indirect mediator species effects with graphical models. *Methods in Ecology*
872 *and Evolution*, *10*(9), 1571–1583.
873 R Core Development Team. (2019). *R: A language and environment for statistical computing*.
874 Roderick, G. K., Croucher, P. J. P., Vandergast, A. G., & Gillespie, R. G. (2012). Species Differentiation on a
875 Dynamic Landscape: Shifts in Metapopulation Genetic Structure Using the Chronology of the
876 Hawaiian Archipelago. *Evolutionary Biology*, *39*(2), 192–206. https://doi.org/10.1007/s11692-
877 012-9184-5
878 Rominger, A. J., Goodman, K. R., Lim, J. Y., Armstrong, E. E., Becking, L. E., Bennett, G. M., Brewer, M. S.,
879 Cotoras, D. D., Ewing, C. P., Harte, J., Martinez, N. D., O'Grady, P. M., Percy, D. M., Price, D. K.,
880 Roderick, G. K., Shaw, K. L., Valdovinos, F. S., Gruner, D. S., & Gillespie, R. G. (2016). Community

assembly on isolated islands: Macroecology meets evolution. *Global Ecology and Biogeography*, *25*(7), 769–780. https://doi.org/doi:10.1111/geb.12341

Rosindell, J., Hubbell, S. P., & Etienne, R. S. (2011). The Unified Neutral Theory of Biodiversity and Biogeography at Age Ten. *Trends in Ecology & Evolution*, *26*(7), 340–348. https://doi.org/10.1016/j.tree.2011.03.024

Rosindell, J., & Phillimore, A. B. (2011). A unified model of island biogeography sheds light on the zone of radiation. *Ecology Letters*, *14*(6), 552–560. https://doi.org/10.1111/j.1461-0248.2011.01617.x

Segar, S. T., Fayle, T. M., Srivastava, D. S., Lewinsohn, T. M., Lewis, O. T., Novotny, V., Kitching, R. L., & Maunsell, S. C. (2020). The role of evolution in shaping ecological networks. *Trends in Ecology & Evolution*, *35*(5), 454–466.

Shaw, & Gillespie, R. G. (2016). Comparative phylogeography of oceanic archipelagos: Hotspots for inferences of evolutionary process. *Proceedings of the National Academy of Sciences*, *113*(29), 7986–7993. https://doi.org/10.1073/pnas.1601078113

Sievers, F., Wilm, A., Dineen, D., Gibson, T. J., Karplus, K., Li, W., Lopez, R., McWilliam, H., Remmert, M., & Söding, J. (2011). Fast, scalable generation of high-quality protein multiple sequence alignments using Clustal Omega. *Molecular Systems Biology*, *7*(1), 539.

Simberloff. (2006). Invasional meltdown 6 years later: Important phenomenon, unfortunate metaphor, or both? *Ecology Letters*, *9*(8), 912–919.

Simberloff, D. S., & Von Holle, B. (1999). Positive interactions of nonindigenous species: Invasional meltdown? *Biological Invasions*, *1*(1), 21–32.

Smith-Ramesh, L. M., Moore, A. C., & Schmitz, O. J. (2017). Global synthesis suggests that food web connectance correlates to invasion resistance. *Global Change Biology*, *23*(2), 465–473. https://doi.org/10.1111/gcb.13460

Stachowicz, J. J., & Hay, M. E. (1999). Reducing predation through chemically mediated camouflage: Indirect effects of plant defenses on herbivores. *Ecology*, *80*(2), 495–509.

Staniczenko, Lewis, O. T., Tylianakis, J. M., Albrecht, M., Coudrain, V., Klein, A.-M., & Reed-Tsochas, F. (2017). Predicting the effect of habitat modification on networks of interacting species. *Nature Communications*, *8*(1), 1–10.

Staniczenko, P. P., Kopp, J. C., & Allesina, S. (2013). The ghost of nestedness in ecological networks. *Nature Communications*, *4*(1), 1–6.

Staniczenko, P. P., Lewis, O. T., Jones, N. S., & Reed-Tsochas, F. (2010). Structural dynamics and robustness of food webs. *Ecology Letters*, *13*(7), 891–899.

Trøjelsgaard, K., Báez, M., Espadaler, X., Nogales, M., Oromí, P., Roche, F. L., & Olesen, J. M. (2013). Island biogeography of mutualistic interaction networks. *Journal of Biogeography*, *40*(11), 2020–2031.

Trøjelsgaard, K., & Olesen, J. M. (2016). Ecological networks in motion: Micro- and macroscopic variability across scales. *Functional Ecology*, *30*(12), 1926–1935. https://doi.org/10.1111/1365-2435.12710

Tylianakis, J. M., Tscharntke, T., & Lewis, O. T. (2007). Habitat modification alters the structure of tropical host–parasitoid food webs. *Nature*, *445*(7124), 202–205. https://doi.org/10.1038/nature05429

Vacher, C., Daudin, J.-J., Piou, D., & Desprez-Loustau, M.-L. (2010). Ecological integration of alien species into a tree-parasitic fungus network. *Biological Invasions*, *12*(9), 3249–3259.

Vacher, C., Tamaddoni-Nezhad, A., Kamenova, S., Peyrard, N., Moalic, Y., Sabbadin, R., Schwaller, L., Chiquet, J., Smith, M. A., & Vallance, J. (2016). Learning ecological networks from next-generation sequencing data. *Advances in Ecological Research*, *54*, 1–39.

Vázquez, D. P., & Aizen, M. A. (2006). Community-wide patterns of specialization in plant–pollinator interactions revealed by null models. *Plant–Pollinator Interactions: From Specialization to Generalization*, 200–219.

Vázquez, D. P., Melián, C. J., Williams, N. M., Blüthgen, N., Krasnov, B. R., & Poulin, R. (2007). Species abundance and asymmetric interaction strength in ecological networks. *Oikos*, *116*(7), 1120–1127. https://doi.org/10.1111/j.0030-1299.2007.15828.x

Venturelli, O. S., Carr, A. V., Fisher, G., Hsu, R. H., Lau, R., Bowen, B. P., Hromada, S., Northen, T., & Arkin, A. P. (2018). Deciphering microbial interactions in synthetic human gut microbiome communities. *Molecular Systems Biology*, *14*(6), e8157.

Vitousek, P. M. (2002). Oceanic islands as model systems for ecological studies. *Journal of Biogeography*, *29*(5–6), 573–582.

Walker, L. R., Wardle, D. A., Bardgett, R. D., & Clarkson, B. D. (2010). The use of chronosequences in studies of ecological succession and soil development. *Journal of Ecology*, *98*(4), 725–736.

Weber, M. G., Wagner, C. E., Best, R. J., Harmon, L. J., & Matthews, B. (2017). Evolution in a Community Context: On Integrating Ecological Interactions and Macroevolution. *Trends in Ecology & Evolution*, *32*(4), 291–304. https://doi.org/10.1016/j.tree.2017.01.003

Wei, Z., Yang, T., Friman, V.-P., Xu, Y., Shen, Q., & Jousset, A. (2015). Trophic network architecture of root-associated bacterial communities determines pathogen invasion and plant health. *Nature Communications*, *6*(1), 8413. https://doi.org/10.1038/ncomms9413

Wolfe, E. W., & Morris, J. (1996). *Geologic map of the Island of Hawaii*. US Geological Survey.

Yeakel, J. D., Pires, M. M., Rudolf, L., Dominy, N. J., Koch, P. L., Guimarães, P. R., & Gross, T. (2014). Collapse of an ecological network in Ancient Egypt. *Proceedings of the National Academy of Sciences*. https://doi.org/10.1073/pnas.1408471111

Yu, D. W., Ji, Y., Emerson, B. C., Wang, X., Ye, C., Yang, C., & Ding, Z. (2012). Biodiversity soup: Metabarcoding of arthropods for rapid biodiversity assessment and biomonitoring. *Methods in Ecology and Evolution*, *3*(4), 613–623.

Zhang, Kobert, K., Flouri, T., & Stamatakis, A. (2014). PEAR: A fast and accurate Illumina Paired-End reAd mergeR. *Bioinformatics*, *30*(5), 614–620.

Zimmerman, E. C. (1970). Adaptive Radiation in Hawaii with Special Reference to Insects. *Biotropica*, *2*(1), 32–38. https://doi.org/10.2307/2989786

Data Accessibility

Data are deposited in a Dryad data repository at https://doi.org/10.6078/D1DX4T and code is hosted on Zenodo at https://zenodo.org/record/7349067 including: 1) DNA sequence data (fasta files) from whole organism community metabarcoding and the DNA barcode reference library, and 2) processed data used in these analyses including the OTU table, phylogenetic species ids, NIClassify predictions, and geographic information.

Author Contributions

967 N.R.G., D.S.G, R.G.G., H.K., J.Y.L. designed the research, N.R.G. and H.K. performed molecular
968 processing of the samples, N.R.G. and P.S. analyzed the data, J.C. and J.C.A. contributed new analytical
969 tools, N.R.G. and R.G.G. wrote the manuscript with input and comments from all coauthors.

970

971 **Tables and Figures**

972 **Table 1: Some expectations for network structure in response to ecological and evolutionary**
973 **factors influencing community assembly through time.** Specialization should change at the network
974 level to depict the changes at the taxon level of more evolved associations. Since the associations of
975 each species are becoming more specialized there is an expectation that an individual taxon will have
976 fewer interactions and the makeup of the whole community will have more interactions overall. [1]
977 (Bufford et al., 2020) [2] (Vázquez et al., 2007) [3] (Tylianakis et al., 2007) [4] (Peralta et al., 2014) [5]
978 (Coux et al., 2016) [6] (Ponisio et al., 2019) [7] (Segar et al., 2020) [8] (Chamberlain et al., 2014) [9]
979 (Blüthgen et al. 2006) [10] (Dunne & Williams, 2009)
980

Process	Richness?	Specialization?	e.g., metric change	Expected change in metric through extended period of community assembly
Immigration	↑	-	Connectance	Connectance should increase in response to immigration when generalist colonists take advantage of weak resource defenses, increasing the number of associations that form out of all possible associations [1]
Environmental filtering	↓	↑	Linkage Density	Linkage density should be higher in novel (young or recently disturbed) networks due to generalists with a greater number of interactions per species [1]
Increasing abundance	↑↓	-	Interaction Evenness	Interaction evenness should decrease with dynamics in taxon abundance because skewed frequency distributions (i.e., a few species with many links and many species with few links) are largely driven by species abundance [2]
Antagonistic interactions	↑↓	↑	Vulnerability	Vulnerability is high in highly modified systems [3] because the average number of consumers per resource is high. Thus, we expect vulnerability to be high in the very youngest community forming on bare lava and go down. However, we expect vulnerability will increase over long temporal scales with reduced competition, predation, parasitism, etc. leading to some level of resource redundancy, for example several species feed on the same resource.
Beneficial interactions	↑	↑	Generality	Generality should increase with increasing pollination, frugivory, camouflage, etc. because species can share the same resources in different locations or times resulting in resource complementarity. [4]
Increasing niches	↑	↑	Generality, Vulnerability	The narrowing of interactions to a subset of resources increases specialization. [5] As niches proliferate the fraction of species associations per interaction partner will go down, e.g., niche breadth of herbivores decreased with island age. [6]
Trait diversification	↑	↑	Linkage Density, H_2'	Evolution and network structure are linked [7]. For example, traits with a phylogenetic signal (such as flower symmetry and pollinator size) can accurately predict interaction partners. [8] If species traits diversify together (co-evolve) then more one-to-one relationships will result in lower linkage density and higher specialization (H_2').
Speciation	↑	↑	Interaction Evenness	Where food webs are dominated by a single link interaction evenness is lowest. [3] With the addition of species through *in situ* speciation, the number of links will increase with greater interaction evenness.
Extinction	↓	↓	Connectance	A specialist species may go extinct from the loss of an essential resource. Species interaction networks composed of many specialist species should have low connectance, and primary extinctions are expected to propagate quickly. [9]

981

982

983 **Table 2. Binary and Weighted network summary statistics.** Metrics calculated from binary (i.e.
984 unweighted, presence-absence) matrices are easily interpretable but sensitive to sampling differences
985 (Banašek-Richter et al., 2004). Quantitative versions based on information theory are more conservative
986 when comparing differences among sites. Each metric incorporates the diversity of individuals comprising
987 the resource (H_N, the diversity of inflows) and of that going to the consumers (H_P, the diversity of outflows)
988 for each species *k*. The quantitive metrics are then based on the reciprocals of these Shannon Entropy
989 values ($n_{N,k}$, and $n_{p,k}$, respectively). The notation q is applied to the quantitive version of that metric. All
990 equations and notations reference [1] (Bersier et al., 2002) [2] (Tylianakis et al., 2007) [3] (Blüthgen et al.
991 2006).
992

Summary statistic		Equation or notation	Description
Number of nodes	B	S = R+C	Total number of species (S) or 'nodes' is equal to the number of prey or resource species (R; lower-level) plus the number of consumer species (C; upper-level)
Number of links	B	L	Total number of interactions or 'links'
Ratio resource: consumers	B	R/C [1]	Average number of resource species per consumer species
Diversity of inflows	W	$H_{N,k}$, (5) [1]	Shannon entropy of weights for a given consumer sp.
Diversity of outflows	W	$H_{P,k}$, (6) [1]	Shannon entropy of weights for a given resource sp.
Log-reciprocal of (5)	W	$n_{N,k}$, (7) [1]	Effective number of resource spp. for a given consumer sp.
Log-reciprocal of (6)	W	$n_{p,k}$, (8) [1]	Effective number of consumer spp. for a given resource sp.
Link density	B	LD = L/S [1]	Average number of interactions per species
	W	LD_q, (14) [1]	weighted version
Connectance	B	Conn = L/(RxC) [1]	Proportion of realized links
	W	$Conn_q = LD_q/S$ [1]	weighted version
Generality	B	G = L/C [1]	Average number of resource sp. per consumer sp.
	W	G_q, (25) [1]	weighted version
Vulnerability	B	V = L/R [1]	Average number of consumer sp. per resource sp.
	W	V_q, (27) [1]	weighted version
Interaction evenness	W	I.E. [2]	Shannon entropy of interaction weights
Index of specialization	W	H2' [3]	Ranges between 0 and 1.0 for extreme generalization and specialization, respectively

993

994

995 **Table 3. Spearman's correlation tests for network metrics and community age.**
996 Spearman's correlation tests were used to determine the significance of the relationship between each
997 quantitative network metric value and ln substrate age (community age). Graphs of regressions in Figure
998 4.

	S	p-value	Spearman's rho
Quantitative (weighted) x community age			
linkage density	76	0.033	0.65
weighted connectance	154	0.371	0.30
generality	124	0.183	0.44
vulnerability	80	0.040	0.64
interaction evenness	70	0.025	0.68
index of specialization H_2'	134	0.237	0.39

999

1000

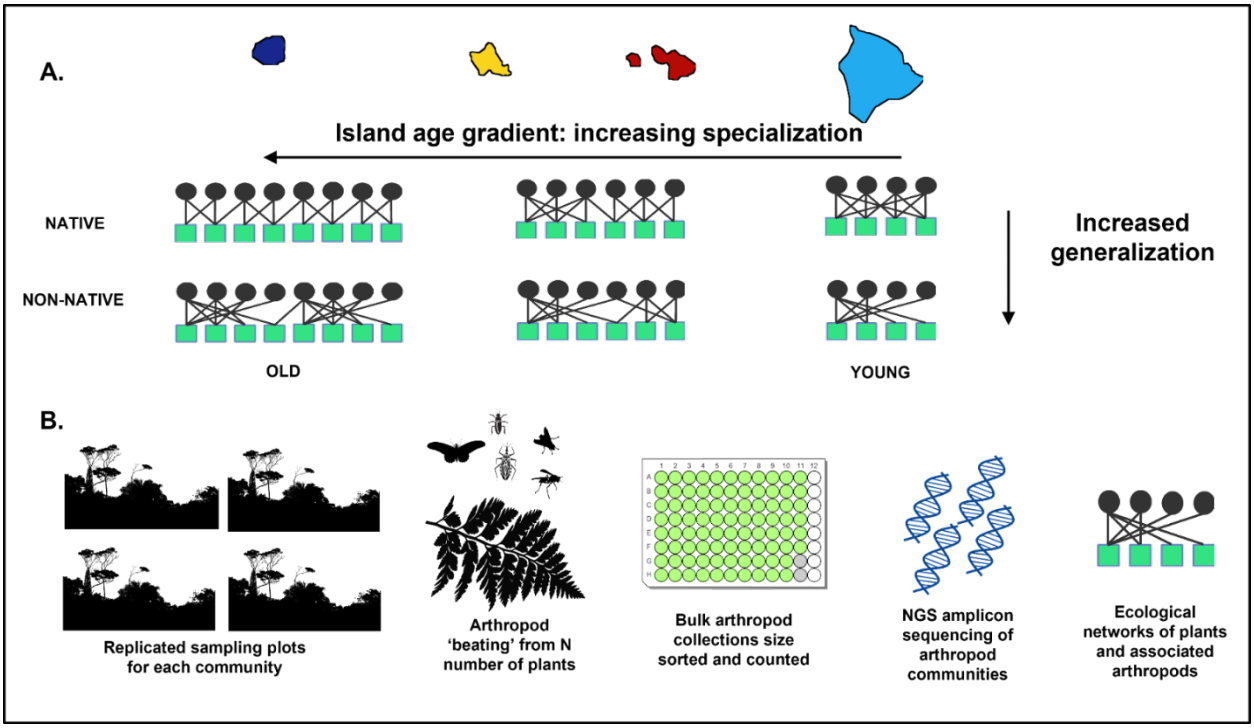

Figure 1. Study overview. A) *Study aims.* As communities assemble over time species will be added through ecological and evolutionary processes. Network size will increase over time. There will be a trend towards greater specialization as relationships among species are modified through ecological fitting and evolutionary adaptation over extended time, young to old sites (top panel). Recently introduced species (i.e., non-natives) evolved elsewhere and have not adapted in place to biotic and abiotic factors, thus limiting their specialization within communities at all stages of development (bottom panel). B) *Study design.* Within multiple 15 m radius plots at 11 communities from ages 50 y to 4.15 Myr plant species were sampled for associated arthropods by vegetation beating according to their relative abundance. Each sample of plant-associated arthropods was size sorted, counted, and placed into a well of a 96-well plate, such that well 'A1' contained sample 1, size category 0-2 mm, and well 'A2' contained sample 1, size category 2-4mm, and so on. DNA extraction and PCR amplification with dual-indexing was used to prepare the size-sorted samples into amplicon libraries which were sequenced on an Illumina Miseq® for the cytochrome oxidase I locus. Ecological networks were constructed from the arthropod-plant associations for each community age.

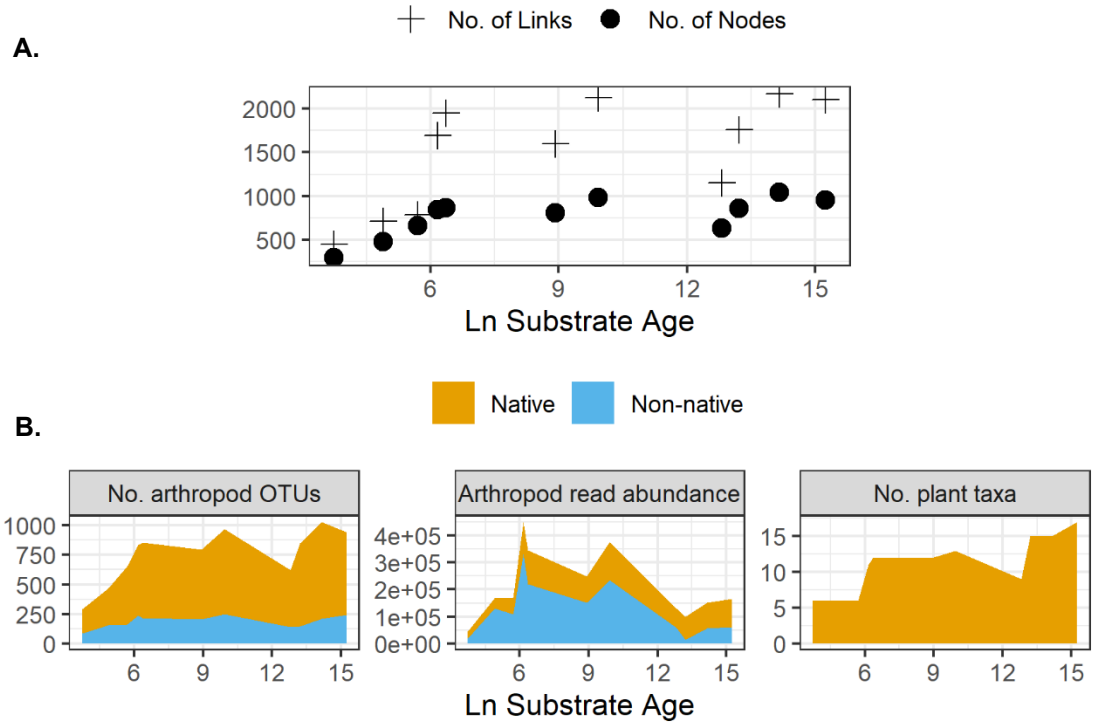

Figure 2. Effect of community assembly over evolutionary time on network size and diversity of native and non-native taxa. A) The number of nodes (arthropod and plant richness) and the number of links (arthropod-plant associations) significantly increase in concert with community age. Spearman's correlation test values SI Table 4. B) Native arthropod richness increases, while non-native richness does not increase, with community age. C) Abundance of native and non-native arthropod species peaks at middle-aged communities but the abundance of non-native taxa is proportionately higher in the youngest communities. D) Native plant richness increases with community age.

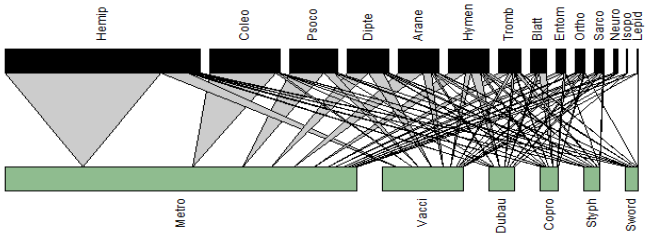

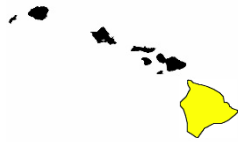

Kilauea: 1973 lava flow 50 yo

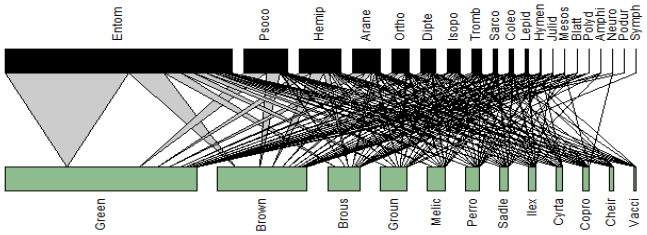

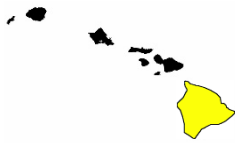

Mauna Loa: Olaa 7,500 yo

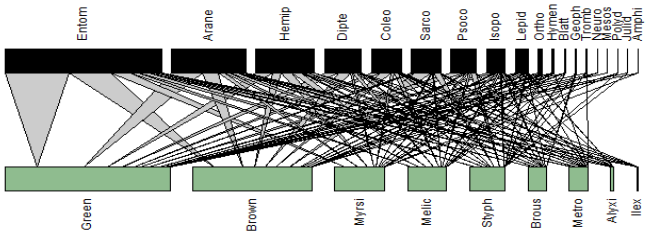

Kohala: Kohala 365,000 yo

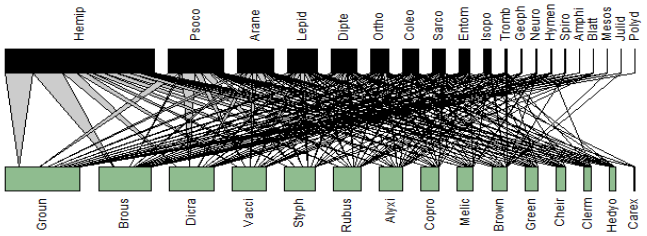

Maui: Waikamoi 545,000 yo

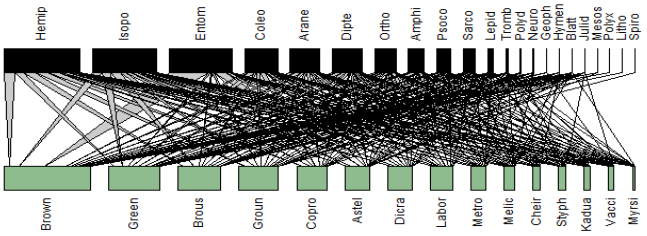

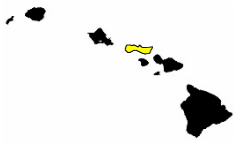

Molokai: Kamakou 1.4 myo

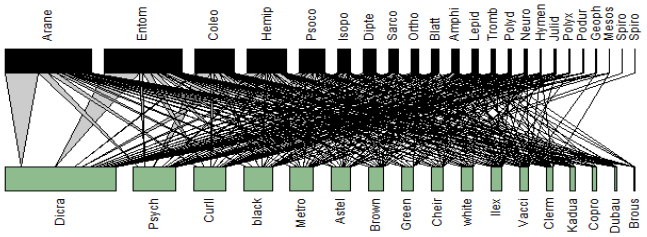

Kauai: Kokee 4.15 myo

Figure 3. Quantitative arthropod–plant networks along a gradient of increasing community assembly (top to bottom). For each network, lower bars represent plant abundance based on sampling time and upper bars represent arthropod abundance based on OTU frequency. Each network is plotted in order of the most abundant taxa from left to right so that the turnover in arthropod-plant association can be seen for each community. Linkage width indicates the frequency of each association as measured using arthropod read abundance. As a summary, the networks show interaction data pooled across all plots for each community age with OTUs pooled by arthropod order, but analyses were performed at the OTU per plant genus level. The bipartite graphs from each of the 11 sampled sites are in SI Figure 3. Arthropod and plant id codes are given in SI Table 3.

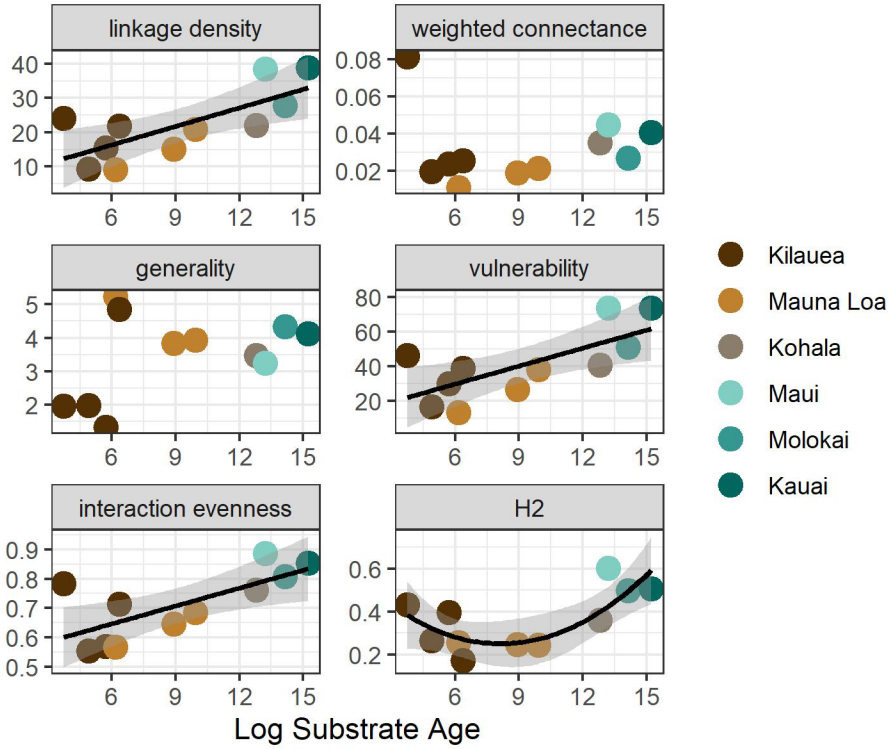

Figure 4. The effect of community age on quantitative ecological network metrics. Statistical measures of network architecture indicating changes in arthropod-plant associations in concert with community age. Each network was weighted with the read abundance of the arthropod OTU associated with the plant genus it was collected from, across all plots for a community age. Three metrics show significant relationships with community assembly, increasing over time: linkage density, vulnerability, interaction evenness. Spearman's correlation test values Table 3. Results of the null model analysis for the quantitative ecological networks metrics are presented in SI Figure 6 and SI Table 5. A graph of the results when analyzed for each of the sampled plots within a community age site is presented in SI Figure 7.

MOLECULAR ECOLOGY

Supplemental Information for:

Ecological network structure in response to community assembly processes over evolutionary time

Natalie R. Graham, Henrik Krehenwinkel, Jun Ying Lim, Phillip Staniczenko, Jackson Callaghan, Jeremy C. Andersen, Daniel S. Gruner, Rosemary G. Gillespie

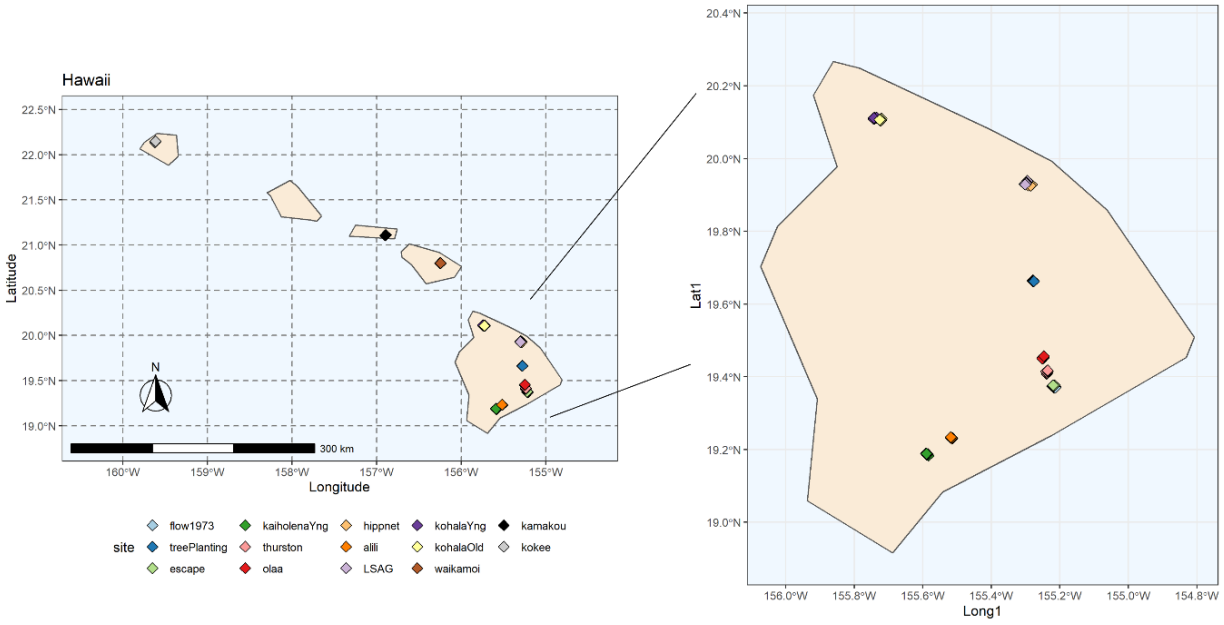

SI Figure 1. Map of sampling sites. 14 sites of varying geologic age were selected, ranging from 50 to 4.15 x 10^6 years old, across four islands of the archipelago: Hawaii, Maui, Molokai, Kauai. To control for climatic differences and disturbance across sites, sites were constrained to ranges of elevation (1000-1300 m) and precipitation (average annual precipitation 2500-3000 mm) and within accessible protected forest lands. See SI Table 2 for substrate age and other site characteristics.

MOLECULAR ECOLOGY

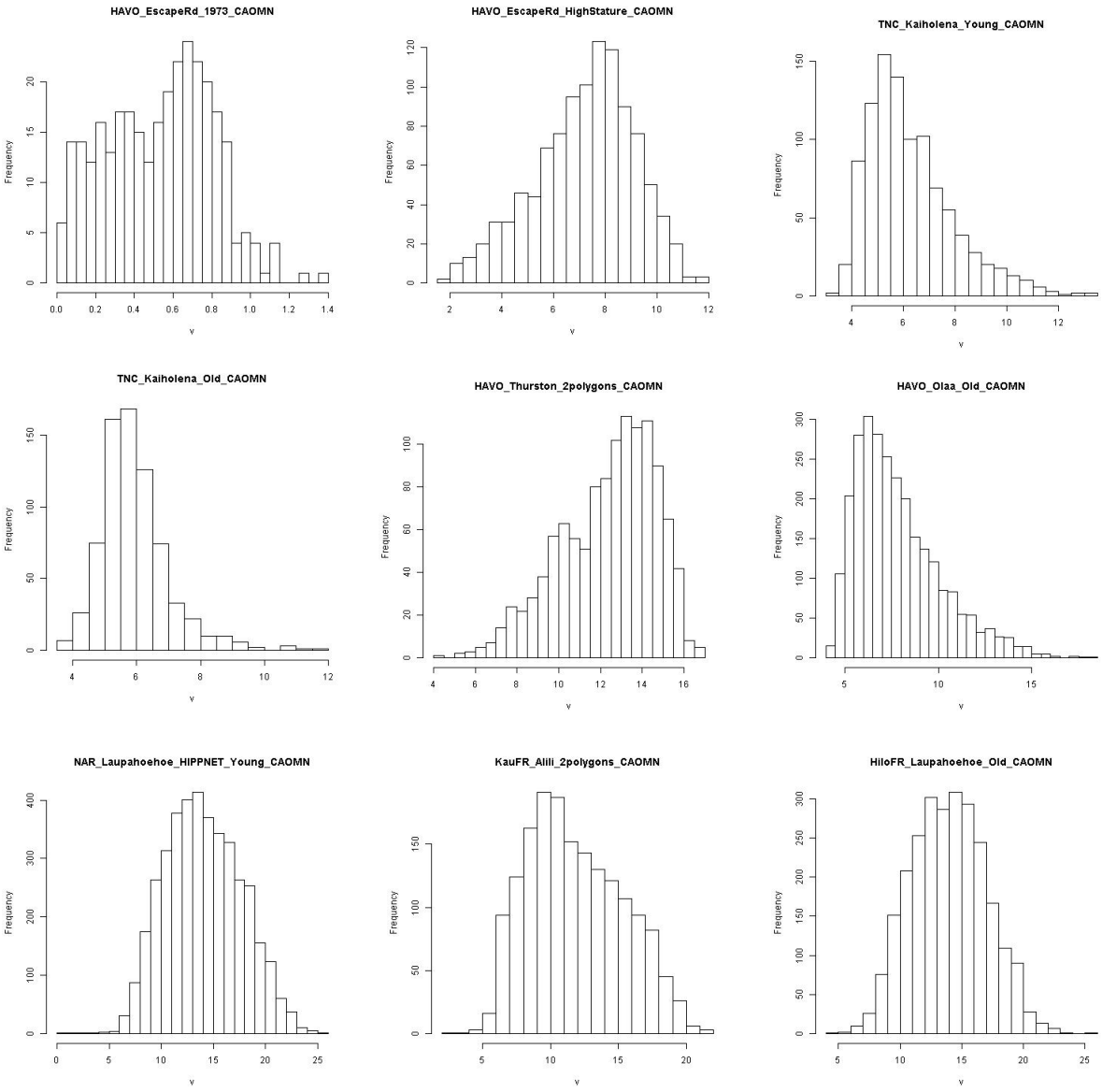

MOLECULAR ECOLOGY

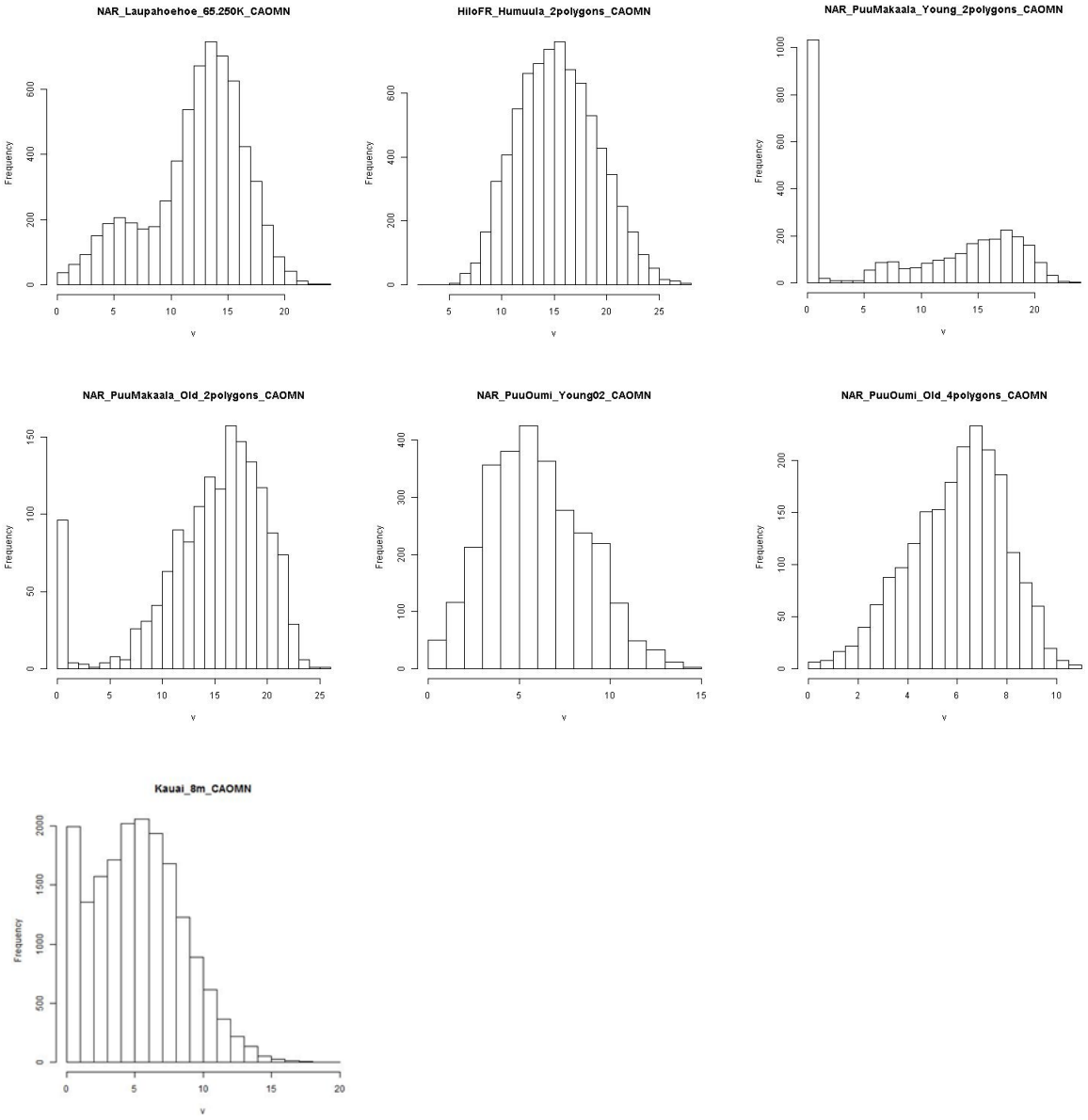

SI Figure 2. Histograms of height profiles from lidar flyover data. Each of the potential sites for the study was assessed for site suitability including these lidar data to evaluate the forest structure. Grain size for lidar was 20 m for all sites except Kauai for which it was 8 m grain size. We used 40% quantile for site comparison because the tails of the distribution of heights was long for some sites, and it would have been difficult to find sites with overlapping height profiles with a more restrictive choice.

MOLECULAR ECOLOGY

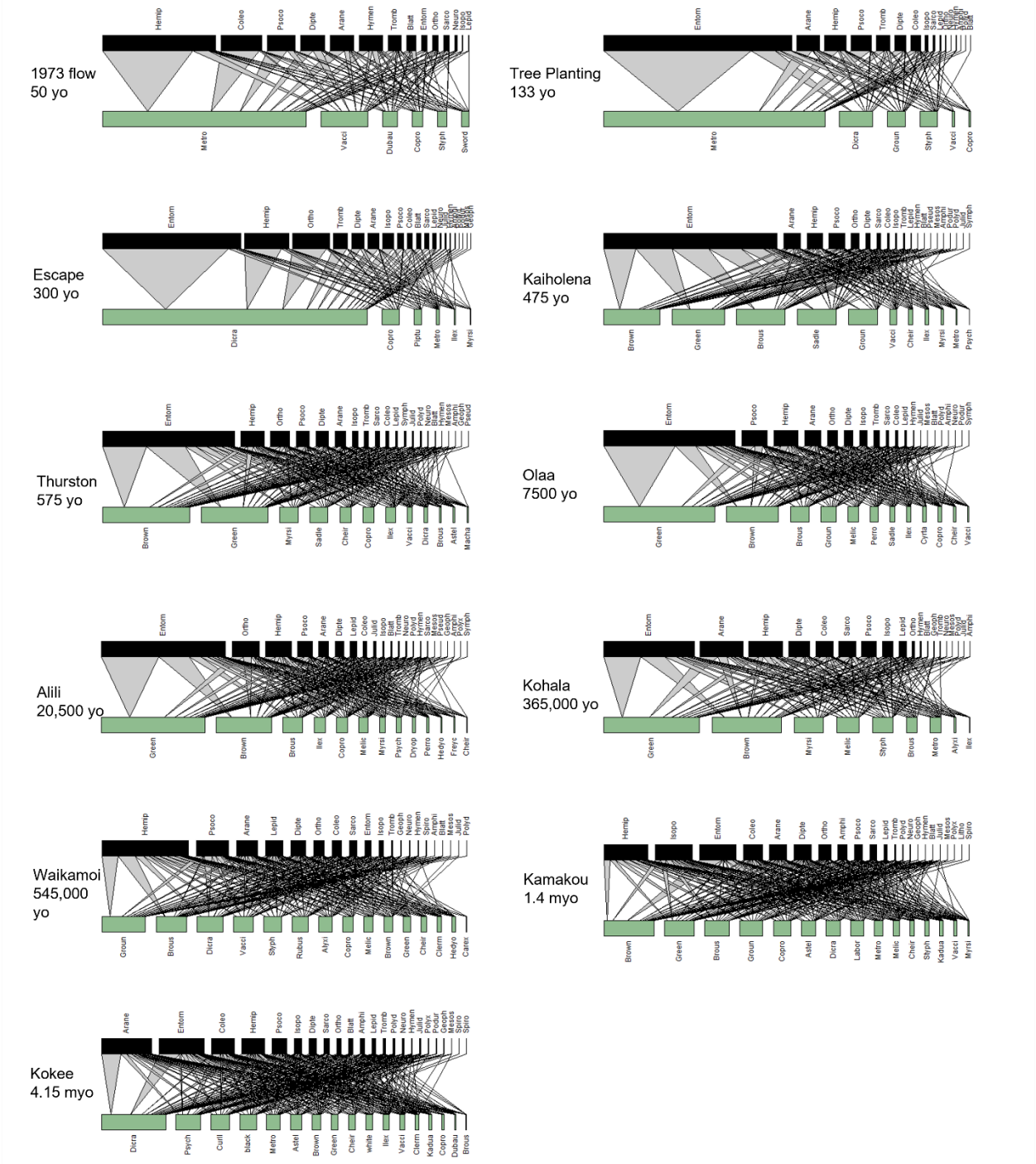

SI Figure 3. Additional bipartite network plots. For each network, lower bars represent plant abundance based on sampling time and upper bars represent arthropod abundance based on OTU

frequency. Each network is plotted in order of the most abundant taxa from left to right so that the turnover in arthropod-plant association can be seen for each community. Linkage width indicates the frequency of each association as measured using arthropod read abundance. As a summary, the networks show interaction data pooled across all plots for each community age with OTUs pooled by arthropod order. However, analyses were performed at the OTU per plant genus level. Arthropod and plant id codes are given in Supplementary Table 1.

MOLECULAR ECOLOGY

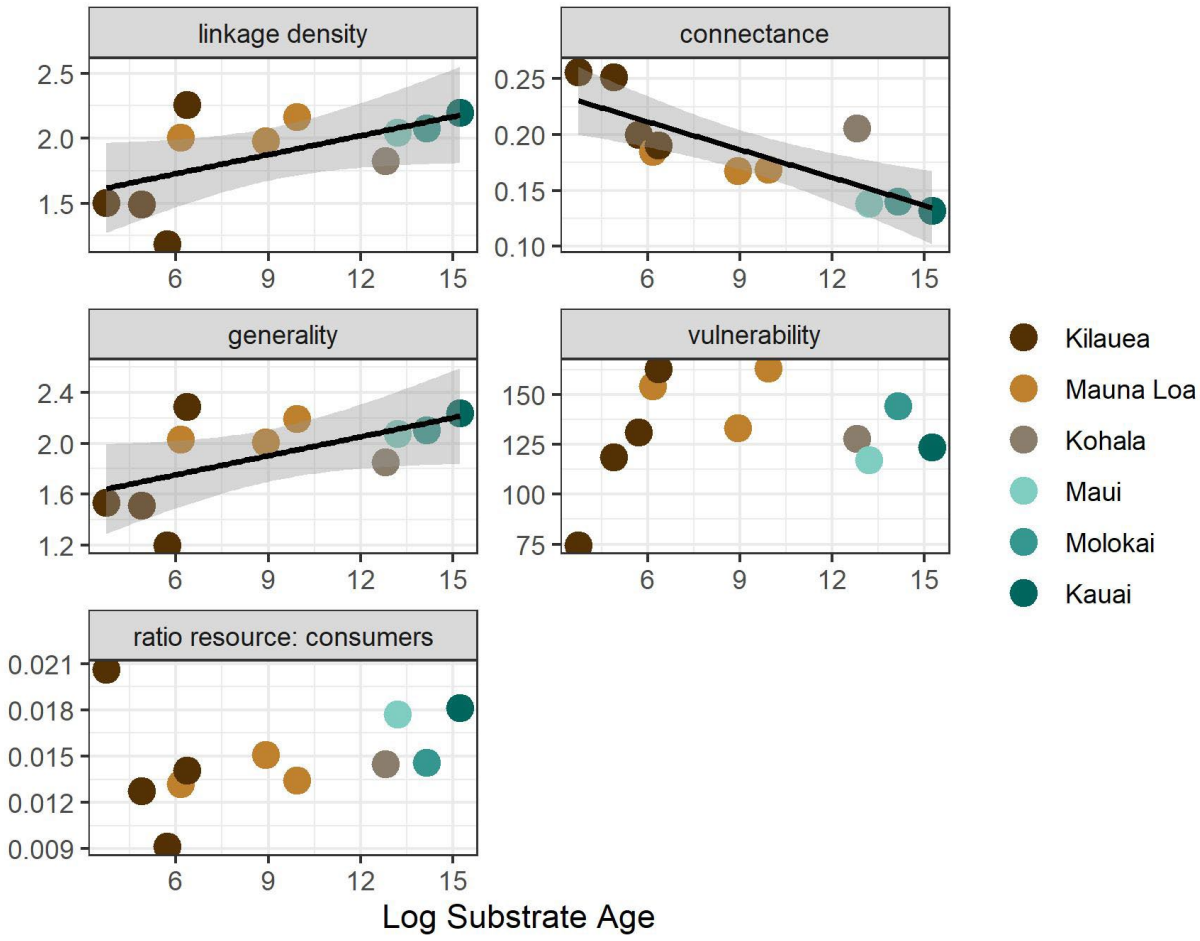

SI Figure 4. The effect of community age on qualitative ecological network metrics. Statistical measures of network architecture were performed using qualitative measures on presence-absence matrices. Three metrics show significant relationships with community age, increasing linkage density and generality and decreasing connectance. Spearman rho and p-values in SI Table 4.

A.

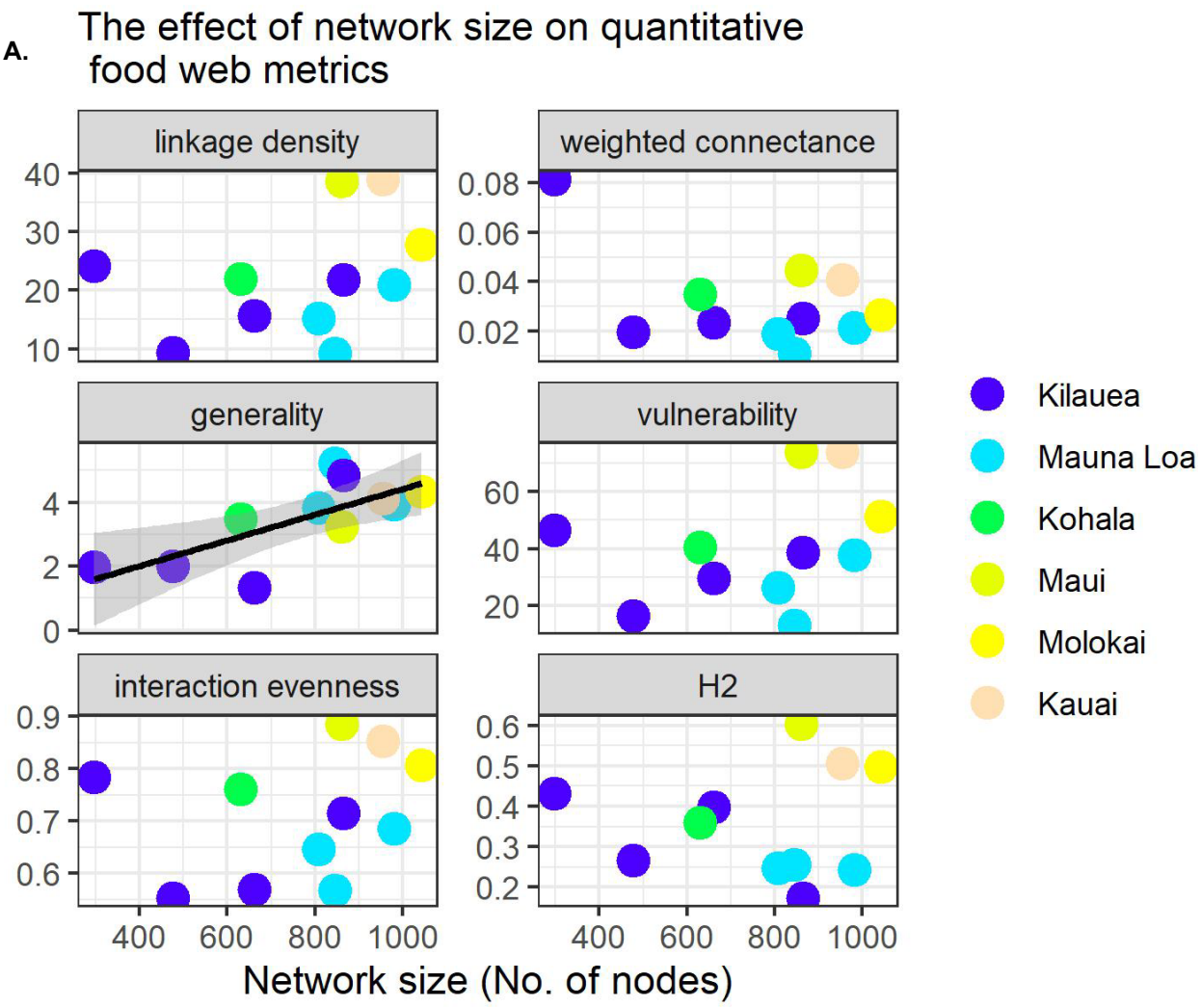
The effect of network size on quantitative food web metrics
linkage density
weighted connectance
generality
vulnerability
interaction evenness
H2
Network size (No. of nodes)
Kilauea
Mauna Loa
Kohala
Maui
Molokai
Kauai

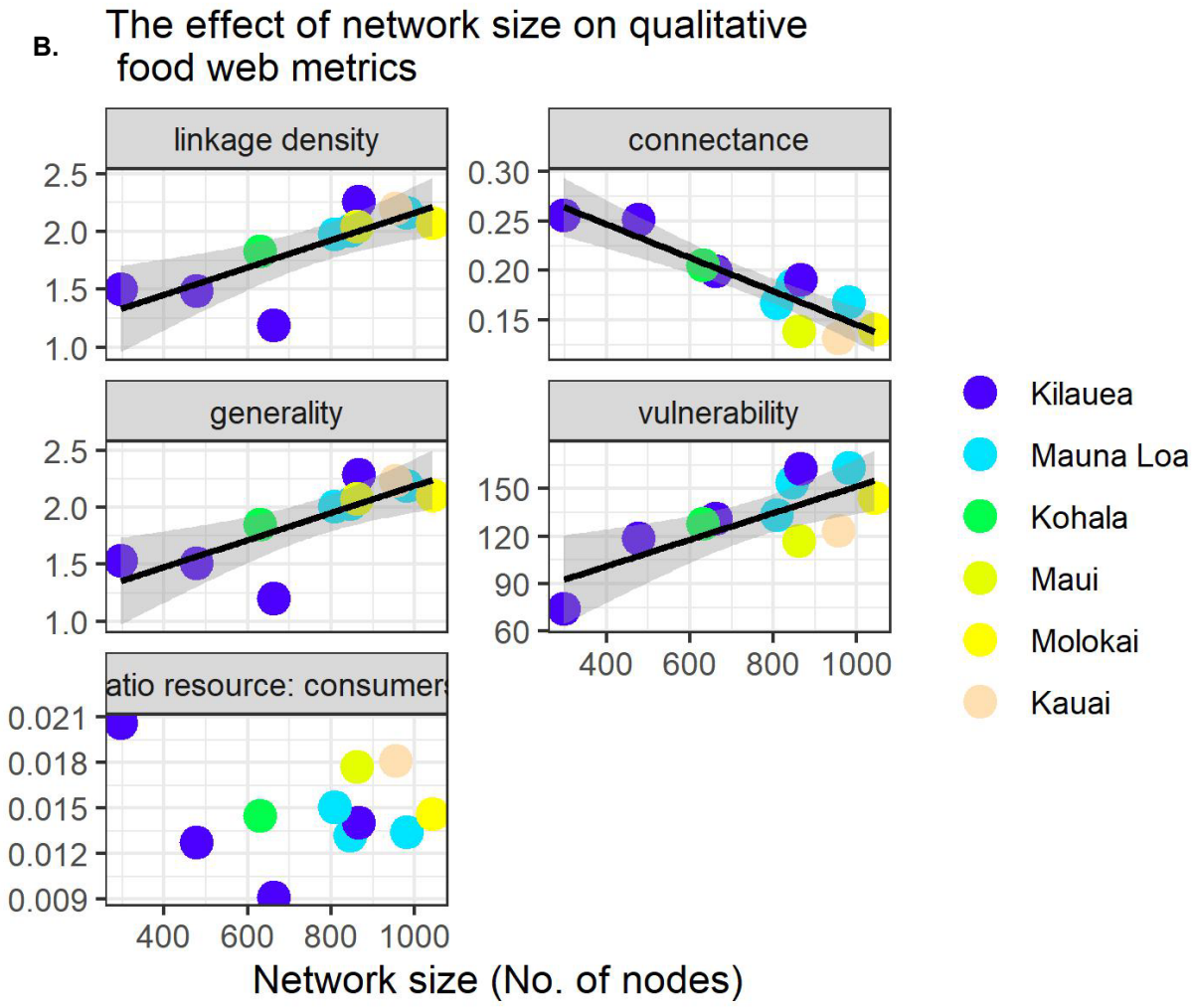

SI Figure 5. The effect of network size on ecological network metrics. Each quantitative and qualitative metrics was regressed against the number of nodes (representing network size). A) Quantitative metrics were not significantly correlated with network size with the exception of generality. B) Qualitative metrics were significantly correlated with network size, with the exception of the ratio of resource:consumers. Spearman rho and p-values in SI Table 4.

MOLECULAR ECOLOGY

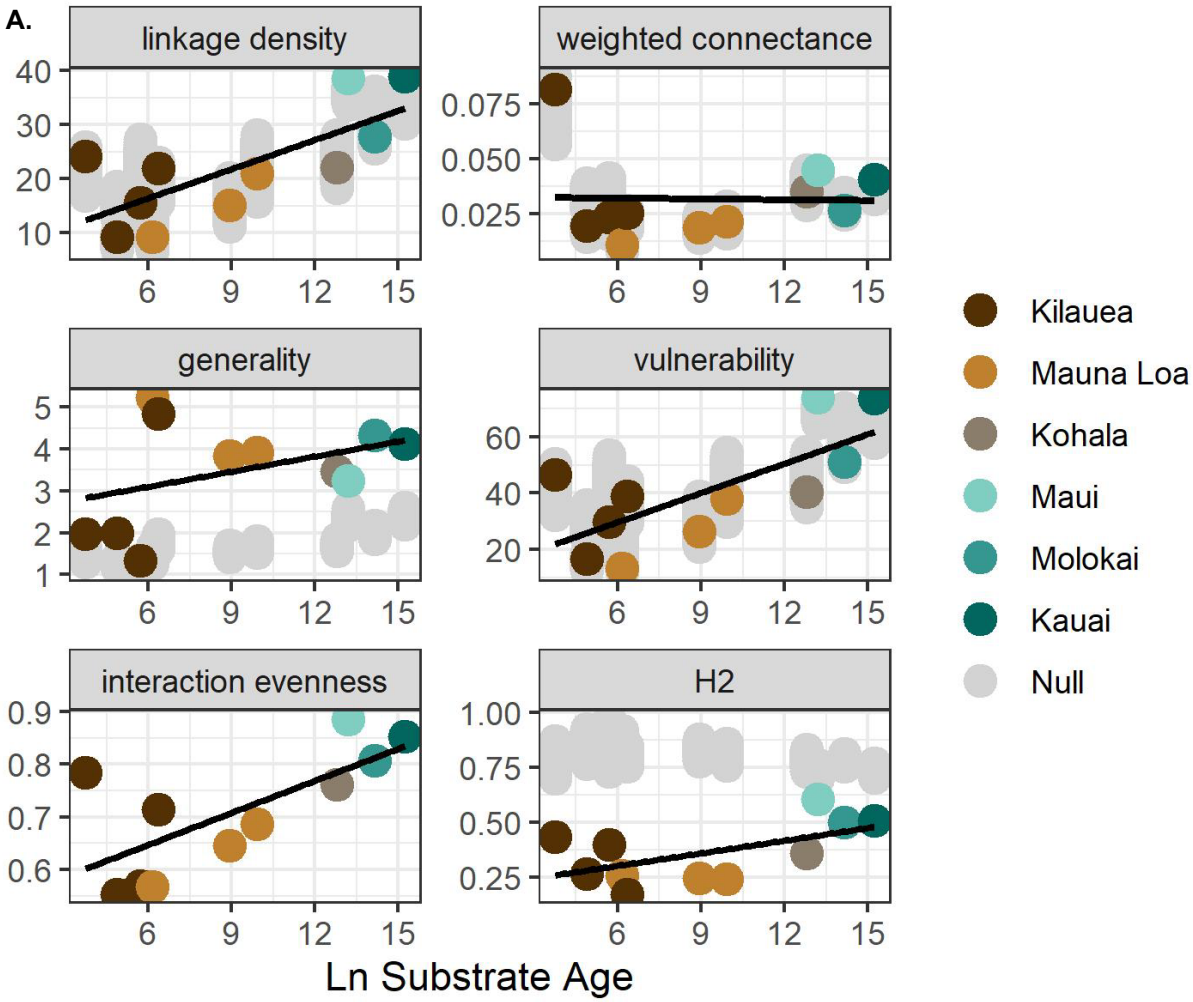

MOLECULAR ECOLOGY

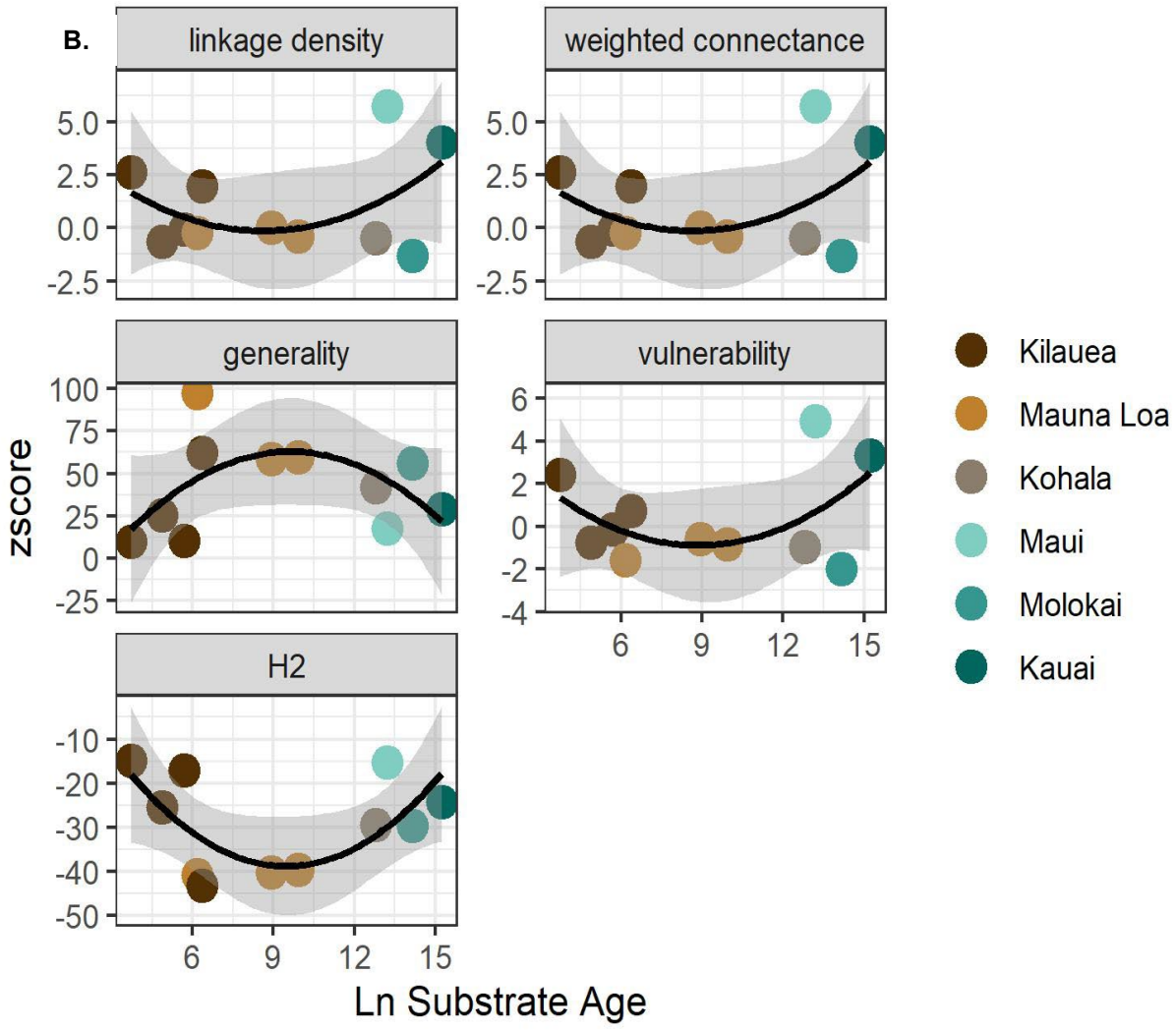

SI Figure 6. Null model analysis for weighted networks. A. Graphs of all 1000 null matrices metric values (gray) and observed values (color) by community age. B. Z-scores from null model analysis of weighted metrics are plotted by community age. There are no null values or z-score for interaction evenness because the null model we used wasn't appropriate given that interaction evenness is based on the empirical distribution of weights, regardless of which species those weights are between.

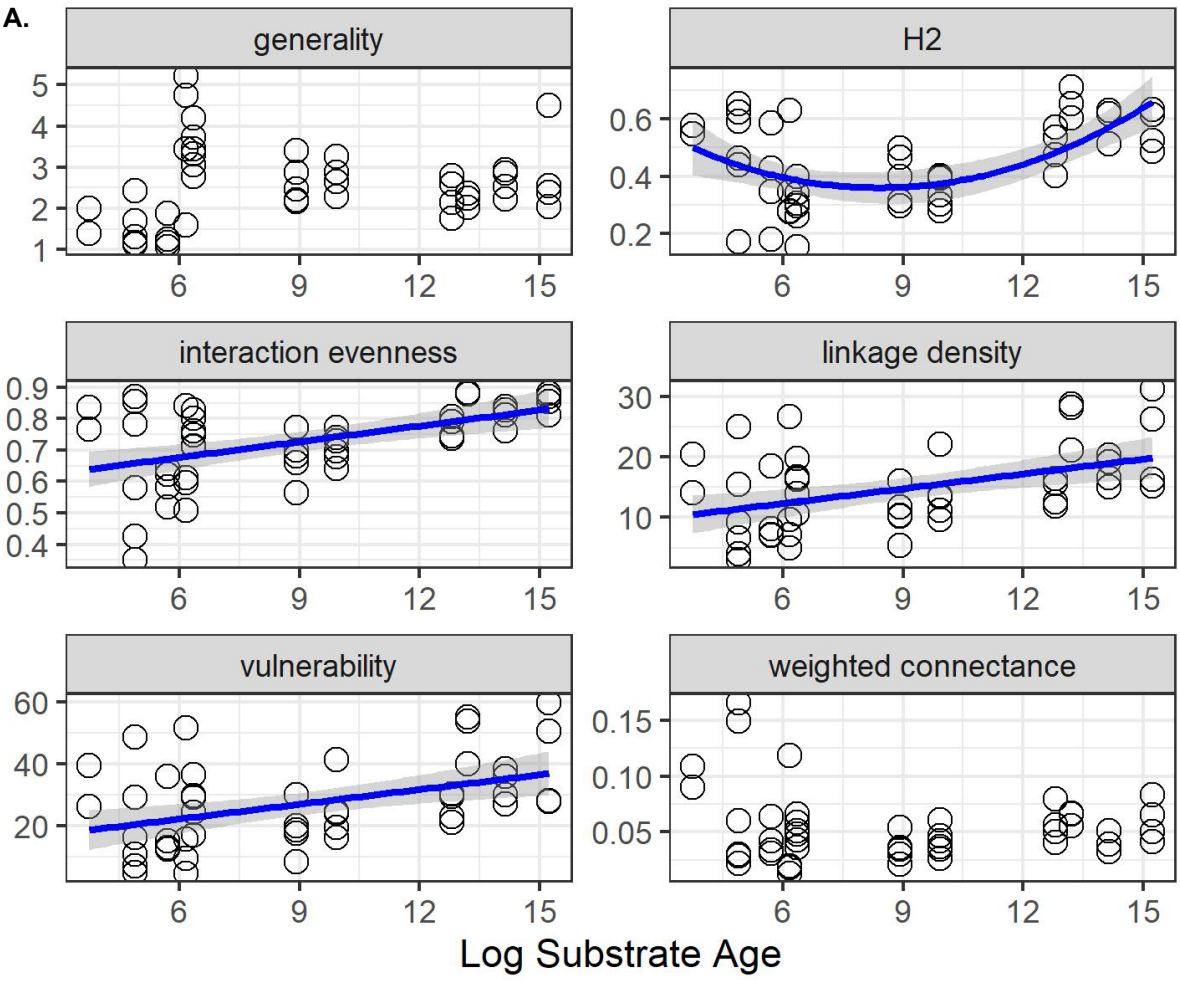
A.
generality
H2
interaction evenness
linkage density
vulnerability
weighted connectance
Log Substrate Age

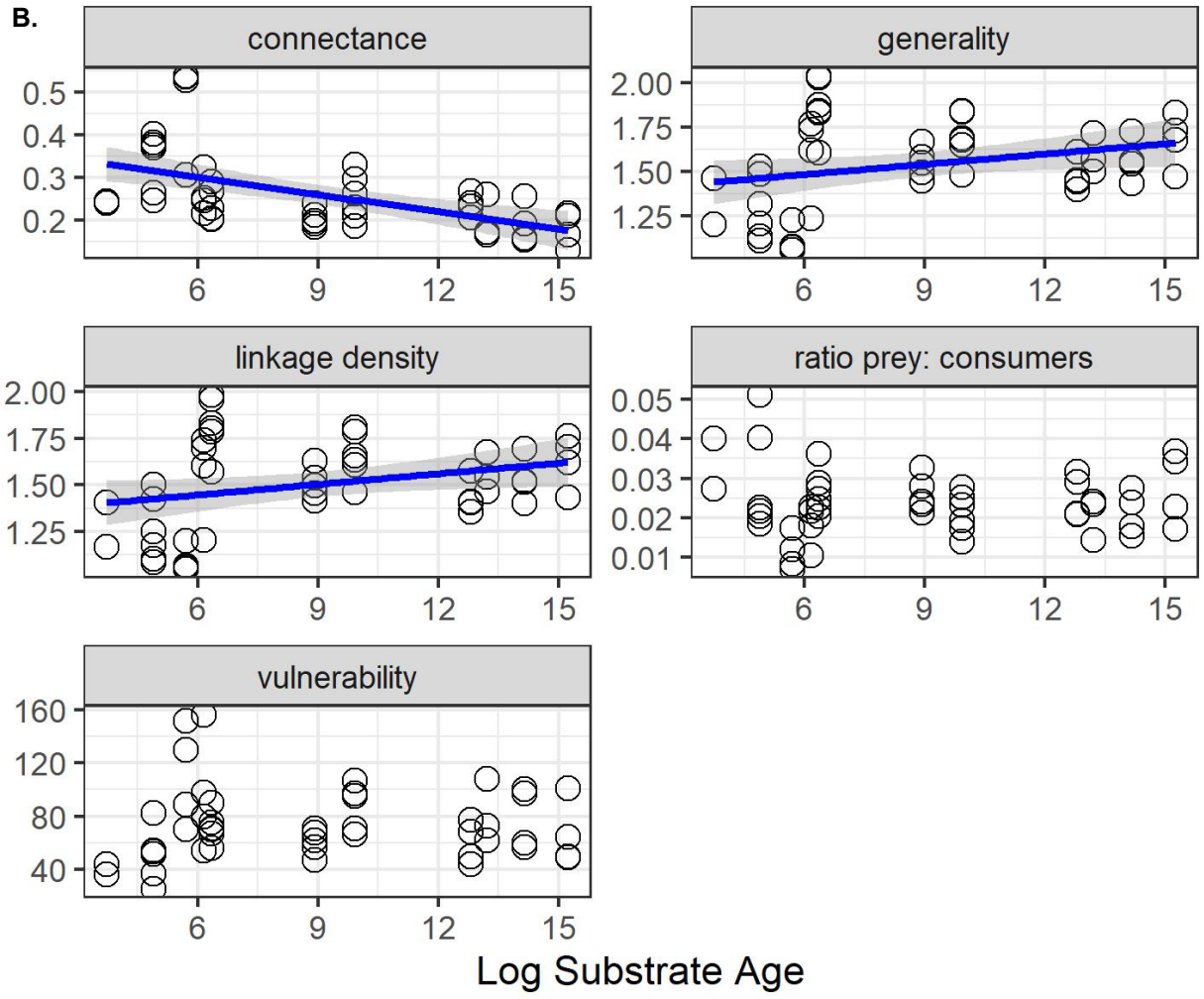

SI Figure 7. Plot level. A. Quantitative and B. Qualitative metrics shown for matrices of arthropod-plant interactions at each plot within a site. In the main text, one network was created per site because our confidence in the network statistics increases with the size of the networks. This was a particular issue for some plots at the youngest and most depauperate sites, where < 4 plant species were sampled within the plot radius and networks would be small. The results from plot level analysis are consistent with the site level data. The variance among plots at the same sites is minimal. These results help corroborate the trend of increasing specialization over time.

MOLECULAR ECOLOGY

SI Table 1. Site information. Information for the sampling plots within each age community. Six plots were sampled in fourteen sites across the island. Plots with greater or less than 1 standard deviation of sample beating time were dropped from analysis. This left a total of 11 sites and 50 plots (highlighted).

Island	Site	Plot	Elev m	AAP m	Lat	Long	Flow age min	Flow age max	Flow age mean
Hawaii	flow1973	flow1973_079	975	2661	19.37	-155.21	42	42	42
Hawaii	flow1973	flow1973_109	975	2613	19.37	-155.22	42	42	42
Hawaii	flow1973	flow1973_084	975	2756	19.37	-155.21	42	42	42
Hawaii	flow1973	flow1973_081	975	2661	19.37	-155.22	42	42	42
Hawaii	flow1973	flow1973_107	975	2570	19.37	-155.22	42	42	42
Hawaii	flow1973	flow1973_110	975	2657	19.37	-155.21	42	42	42
Hawaii	treePlanting	treePlanting_01	1209	4515	19.66	-155.28	133	133	133
Hawaii	treePlanting	treePlanting_03	1204	4495	19.66	-155.28	133	133	133
Hawaii	treePlanting	treePlanting_04	1196	4719	19.66	-155.28	133	133	133
Hawaii	treePlanting	treePlanting_05	1198	4700	19.66	-155.28	133	133	133
Hawaii	treePlanting	treePlanting_02	1198	4515	19.66	-155.28	133	133	133
Hawaii	treePlanting	treePlanting_06	1192	4700	19.66	-155.28	133	133	133
Hawaii	escape	escape_02	997	2658	19.38	-155.22	200	400	300
Hawaii	escape	escape_04	1012	2565	19.37	-155.22	200	400	300
Hawaii	escape	escape_06	1007	2610	19.37	-155.22	200	400	300
Hawaii	escape	escape_87	1004	2748	19.38	-155.22	200	400	300
Hawaii	escape	escape_90	1013	2647	19.38	-155.22	200	400	300
Hawaii	escape	escape_89	1003	2748	19.38	-155.21	200	400	300
Hawaii	kaiholenaYng	kaiholenaYng_02	966	2888	19.18	-155.58	200	750	475
Hawaii	kaiholenaYng	kaiholenaYng_08	1003	2947	19.19	-155.59	200	750	475
Hawaii	kaiholenaYng	kaiholenaYng_09	1045	2937	19.19	-155.59	200	750	475
Hawaii	kaiholenaYng	kaiholenaYng_04	1012	2909	19.19	-155.59	200	750	475
Hawaii	kaiholenaYng	kaiholenaYng_10	1029	2932	19.19	-155.59	200	750	475
Hawaii	kaiholenaYng	kaiholenaYng_11	1045	2926	19.19	-155.59	200	750	475
Hawaii	thurston	thurston_01	1177	2610	19.41	-155.24	400	750	575
Hawaii	thurston	thurston_04	1181	2880	19.41	-155.24	400	750	575
Hawaii	thurston	thurston_05	1189	2838	19.41	-155.24	400	750	575
Hawaii	thurston	thurston_06	1195	2709	19.42	-155.24	400	750	575
Hawaii	thurston	thurston_08	1195	2797	19.42	-155.24	400	750	575
Hawaii	thurston	thurston_12	1189	2850	19.42	-155.24	400	750	575
Hawaii	olaa	olaa_01	1170	3011	19.45	-155.25	5000	10000	7500
Hawaii	olaa	olaa_03	1169	3071	19.45	-155.25	5000	10000	7500
Hawaii	olaa	olaa_06	1177	2957	19.45	-155.25	5000	10000	7500
Hawaii	olaa	olaa_12	1183	2908	19.46	-155.25	5000	10000	7500

Hawaii	olaa	olaa_02	1163	3022	19.45	-155.25	5000	10000	7500
Hawaii	olaa	olaa_10	1183	2915	19.45	-155.25	5000	10000	7500
Hawaii	hippnet	hippnet_05	1131	3538	19.93	-155.28	4000	14000	9000
Hawaii	hippnet	hippnet_06	1152	3506	19.93	-155.29	4000	14000	9000
Hawaii	hippnet	hippnet_08	1126	3654	19.93	-155.28	4000	14000	9000
Hawaii	hippnet	hippnet_09	1212	3318	19.93	-155.29	4000	14000	9000
Hawaii	hippnet	hippnet_11	1231	3295	19.93	-155.29	4000	14000	9000
Hawaii	hippnet	hippnet_13	1177	3479	19.93	-155.29	4000	14000	9000
Hawaii	alili	alili_01	917	2460	19.23	-155.51	11000	30000	20500
Hawaii	alili	alili_04	960	2573	19.23	-155.52	11000	30000	20500
Hawaii	alili	alili_05	917	2504	19.23	-155.52	11000	30000	20500
Hawaii	alili	alili_06	942	2541	19.23	-155.51	11000	30000	20500
Hawaii	alili	alili_14	969	2597	19.23	-155.52	11000	30000	20500
Hawaii	alili	alili_15	985	2583	19.23	-155.52	11000	30000	20500
Hawaii	laupLSAG	laupLSAG_01	1102	3433	19.94	-155.3	14000	65000	39500
Hawaii	laupLSAG	laupLSAG_04	1158	3235	19.94	-155.3	14000	65000	39500
Hawaii	laupLSAG	laupLSAG_07	1155	3235	19.93	-155.3	14000	65000	39500
Hawaii	laupLSAG	laupLSAG_10	1181	3291	19.93	-155.3	14000	65000	39500
Hawaii	laupLSAG	laupLSAG_12	1251	3080	19.93	-155.3	14000	65000	39500
Hawaii	laupLSAG	laupLSAG_15	1242	3112	19.93	-155.3	14000	65000	39500
Hawaii	kohalaYng	kohalaYng_03	1285	2779	20.11	-155.74	120000	230000	175000
Hawaii	kohalaYng	kohalaYng_04	1303	2863	20.11	-155.74	120000	230000	175000
Hawaii	kohalaYng	kohalaYng_07	1274	3004	20.11	-155.74	120000	230000	175000
Hawaii	kohalaYng	kohalaYng_08	1266	3177	20.11	-155.73	120000	230000	175000
Hawaii	kohalaYng	kohalaYng_10	1305	2779	20.11	-155.74	120000	230000	175000
Hawaii	kohalaYng	kohalaYng_20	1281	2918	20.11	-155.74	120000	230000	175000
Hawaii	kohalaOld	kohalaOld_01	1294	3568	20.11	-155.72	230000	500000	365000
Hawaii	kohalaOld	kohalaOld_03	1273	3704	20.11	-155.72	230000	500000	365000
Hawaii	kohalaOld	kohalaOld_08	1313	3402	20.11	-155.73	230000	500000	365000
Hawaii	kohalaOld	kohalaOld_05	1318	3501	20.11	-155.72	230000	500000	365000
Hawaii	kohalaOld	kohalaOld_06	1309	3501	20.11	-155.72	230000	500000	365000
Hawaii	kohalaOld	kohalaOld_07	1335	3419	20.1	-155.72	230000	500000	365000
Maui	waikamoi	waikamoi_07	1591	2518	20.8	-156.25	140000	950000	545000
Maui	waikamoi	waikamoi_16	1545	3040	20.8	-156.24	140000	950000	545000
Maui	waikamoi	waikamoi_36	1564	2765	20.8	-156.25	140000	950000	545000
Maui	waikamoi	waikamoi_06	1547	2834	20.8	-156.25	140000	950000	545000
Maui	waikamoi	waikamoi_18	1552	3107	20.8	-156.24	140000	950000	545000
Maui	waikamoi	waikamoi_32	1524	2598	20.8	-156.25	140000	950000	545000
Molokai	kamakou	kamakou_07	1191	2718	21.11	-156.9	1300000	1500000	1400000
Molokai	kamakou	kamakou_09	1223	3007	21.11	-156.9	1300000	1500000	1400000
Molokai	kamakou	kamakou_17	1213	3007	21.11	-156.89	1300000	1500000	1400000
Molokai	kamakou	kamakou_39	1182	2800	21.11	-156.89	1300000	1500000	1400000

Molokai	kamakou	kamakou_15	1245	3276	21.11	-156.89	1300000	1500000	1400000
Molokai	kamakou	kamakou_41	1159	2532	21.11	-156.9	1300000	1500000	1400000
Kauai	kokee	kokee_16	1116	2251	22.14	-159.62	4000000	4300000	4150000
Kauai	kokee	kokee_21	1200	2860	22.15	-159.62	4000000	4300000	4150000
Kauai	kokee	kokee_23	1210	2877	22.15	-159.61	4000000	4300000	4150000
Kauai	kokee	kokee_11	1147	2487	22.14	-159.62	4000000	4300000	4150000
Kauai	kokee	kokee_09	1172	2413	22.14	-159.62	4000000	4300000	4150000
Kauai	kokee	kokee_22	1202	2724	22.15	-159.62	4000000	4300000	4150000

MOLECULAR ECOLOGY

SI Table 2. Summary statistics from lidar data during site selection. Here we show the basic forest structure characteristics for each of the sites that was characterized as a possible area for arthropod community assessment, The highlighted sites were included for arthropod community assessment using DNA metabarcoding. The sites with NA we did not have lidar data availability.

Site	MEAN	MEDIAN	MIN	MAX	SD	Q40	Kurtosis	KurtSE	Skewness	SkewSE
HAVO_EscapeRd_1973	0.530168	0.563037	0.0099	1.364975	0.274771	0.631655	-0.61762	0.271608	0.044372	0.137784
Tree Planting Road	NA	NA	NA	NA	NA	NA	NA	NA	NA	NA
HAVO_EscapeRd_HighStature	7.21131	7.457712	1.78265	11.91813	1.905806	7.93115	-0.25263	0.14969	-0.42313	0.075164
TNC_Kaiholena_Young	6.254615	5.85335	3.378	13.40897	1.664489	6.35712	1.333989	0.154296	1.105489	0.077498
TNC_Kaiholena_Old	5.928797	5.7883	3.774975	11.6454	1.070454	5.99883	3.697232	0.180073	1.37507	0.090596
HAVO_Thurston	12.37064	12.76153	4.408525	16.77472	2.261814	13.35568	-0.1841	0.141771	-0.61303	0.071156
HAVO_Olaa_Old	7.830925	7.329275	4.076075	18.0546	2.272184	7.9105	0.922662	0.093658	1.041491	0.046906
NAR_Laupahoehoe_HIPPNET	14.05824	13.8389	0.030125	25.2793	3.653928	14.90676	-0.47155	0.077027	0.153058	0.038557
KauFR_Alili	11.86238	11.4214	2.585675	21.81295	3.492847	12.57993	-0.73541	0.118676	0.311218	0.059496
HiloFR_Laupahoehoe_Old	13.94185	13.91757	4.52675	25.16357	3.045798	14.75297	-0.37097	0.096224	0.125453	0.048196
NAR_Laupahoehoe_65-250K	12.23722	13.00572	0.1083	23.588	4.243211	13.84491	-0.04895	0.061824	-0.66387	0.030934
HiloFR_Humuula	15.33543	15.18775	2.23905	27.6691	3.801326	16.22402	-0.40367	0.056136	0.17102	0.028085
NAR_PuuMakaala_Young	5.951452	5.722412	0.14485	14.82202	2.678494	6.496805	-0.37364	0.091493	0.30729	0.045819
NAR_PuuMakaala_Old	14.71206	15.72586	0	25.28247	5.365967	16.84449	1.253179	0.123676	-1.16721	0.062017
NAR_PuuOumi_Young02	5.951452	5.722412	0.14485	14.82202	2.678494	6.496805	-0.37364	0.091493	0.30729	0.045819
NAR_PuuOumi_Old	5.999913	6.243275	0.3082	10.97857	1.918523	6.687105	-0.25813	0.10721	-0.3717	0.053721
Kamakou Molokai	NA	NA	NA	NA	NA	NA	NA	NA	NA	NA
Waikamoi Maui	NA	NA	NA	NA	NA	NA	NA	NA	NA	NA
Kauai_8m	5.248667	5.121489	0.010311	19.3347	3.227693	6.003569	-0.26206	0.036622	0.38	0.018316

MOLECULAR ECOLOGY

SI Table 3. Taxonomic coverage. Taxonomic coverage of arthropod OTUs as determined by percent match to GenBank accessions and a 57 species reference collection. Taxonomy of plants as determined by morphological identification in the field. Plants that were unidentified were grouped by morphotaxa. The bipartite web id is the 5-letter code to match the bipartite plots in Figure 3 and SI Figure 3.

Arthropod Order or Plant Genus/Morphotaxon	otus	species	genus	families	bipartite web id
arthropod molecular taxonomy					
Amphipoda	29		1	1	Amphi
Araneae	539	58	9	8	Arane
Blattodea	12	2	1		Blatt
Coleoptera	421	18	4	12	Coleo
Diptera	454	27	8	19	Dipte
Entomobryomorpha	295	8	3	1	Entom
Geophilomorpha	9				Geoph
Hemiptera	774	37	11	9	Hemip
Hymenoptera	98	12	3	5	Hymen
Isopoda	59	2	2	1	Isopo
Julida	4	3		1	Julid
Lepidoptera	290	18	16	15	Lepid
Lithobiomorpha	1				Litho
Mesostigmata	9	1			Mesos
Neuroptera	30	2	1	2	Neuro
Orthoptera	197	4	2	2	Ortho
Poduromorpha	7		1	1	Podur
Polydesmida	1	1			Polyd
Polyxenida	1				Polyx
Pseudoscorpiones	4				Pseud
Psocoptera	266	4	1		Psoco
Sarcoptiformes	262	1	2		Sarco
Spirobolida	1				Spiro
Spirostreptida	4				Spiro
Symphypleona	4	1	1		Symph
Trombidiformes	14	1		1	Tromb
plant morphological taxonomy					
Metrosideros					Metro
Styphelia					Styph
Vaccinium					Vacci

Swordfern	Sword
Coprosma	Copro
Dubautia	Dubau
Dicranopteris	Dicra
Groundfern	Groun
Myrsine	Myrsi
Pipturus	Piptu
Ilex	Ilex
Broussaisia	Brous
BrownCibotium	Brown
GreenCibotium	Green
Sadleria	Sadle
Cheirodendron	Cheir
Psychotria	Psych
Astelia	Astel
Machaerina	Macha
Melicope	Melic
Perrottetia	Perro
Cyrtandra	Cyrta
Dryopteris	Dryop
Freycinetia	Freyc
Hedyotis	Hedyo
Alyxia	Alyxi
Rubus	Rubus
Clermontia	Clerm
Carex	Carex
Kadua	Kadua
Labordia	Labor
Curlleaf	Curll
whitemid	white
blackvelvet	black

MOLECULAR ECOLOGY

SI Table 4. Spearman's correlation tests. Spearman's correlation tests were used to determine significance for the: A) regression against log substrate age (community age) of qualitative network metric values calculated from binary matrices at each site. B) regression against number of nodes (community size) of quantitative network metric values calculated from weighted matrices at each site C) regression against number of nodes (community size) of qualitative network metric values calculated from binary matrices at each site and D) regression of size of network (number of nodes, number of links) by log flow age (community age).

	S	p-value	Spearman's rho
Qualitative (binary) x community age			
linkage density	78	0.037	0.65
connectance	404	0.003	-0.84
generality	78	0.037	0.65
vulnerability	188	0.670	0.15
ratio prey:consumers	132	0.225	0.40
Quantitative (weighted) x number of nodes			
linkage density	140	0.273	0.36
weighted connectance	226	0.946	-0.03
generality	68	0.023	0.69
vulnerability	144	0.300	0.35
interaction evenness	134	0.237	0.39
index of specialization H_2'	218	0.989	0.01
Qualitative (binary) x number of nodes			
linkage density	34	0.002	0.85
connectance	396	0.005	-0.80
generality	34	0.002	0.61
vulnerability	86	0.051	0.61
ratio prey:consumers	202	0.818	0.08
number of nodes x log flow age	3741	0.000	0.74
number of links x log flow age	3096	0.000	0.78

MOLECULAR ECOLOGY

SI Table 5. p-value table weighted metrics null model analysis. The network metrics of 1000 null matrices were compared to the network metrics of the empirical matrix. The null hypothesis is said to be true if the empirical values are within the null model distribution. This is a two tailed distribution. A "1" indicates that every null model value that we compared to our observed was greater than or equal to the observed value. A "0" indicates that no null model value that we compared to our observed was greater than or equal to the observed value. A value of greater than 0 and less than 1 is simply the number values that the null metric was greater than the empirical metric.

site	pval.Connectance	pval.LD	pval.Gen	pval.Vul	pval.H2
flow1973	0.001	0.001	0	0.006	1
treePlanting	0.518	0.518	0	0.553	1
escape	0.283	0.283	0.002	0.293	1
kaiholenaYng	0.571	0.571	0	0.96	1
thurston	0.031	0.031	0	0.225	1
olaa	0.492	0.492	0	0.645	1
alili	0.596	0.596	0	0.749	1
kohalaOld	0.653	0.653	0	0.825	1
waikamoi	0	0	0	0	1
kamakou	0.889	0.889	0	0.973	1
kokee	0	0	0	0	1